Pleiotropic effects of the vacuolar ABC transporter MLT1 of Candida albicans on cell function and virulence.

Nitesh Kumar Khandelwal, Philipp Kaemmer, T. M. Forster, Ashutosh Singh, Alix T Coste, R. Andes, Bernhard Hube, Dominique Sanglard, Neeraj Chauhan, Rupinder Kaur, et al.

PORTLAND PRESS

BIOCHEMICAL JOURNAL
ACCEPTED MANUSCRIPT

Pleiotropic effects of the vacuolar ABC transporter MLT1 of Candida albicans on cell function and virulence

Nitesh Kumar Khandelwal, Philipp Kaemmer , Toni M. Förster, Ashutosh Singh, Alix T. Coste, David R. Andes, Bernhard Hube, Dominique Sanglard, Neeraj Chauhan , Rupinder Kaur , Christophe d'Enfert, Alok Kumar Mondal, and Rajendra Prasad

Among the several mechanisms that contribute to multidrug resistance (MDR), the overexpression of drug efflux pumps belonging to the ATP-binding cassette (ABC) superfamily is the most frequent cause of resistance to antifungals. The multidrug transporter proteins Cdr1p and Cdr2p of the ABCG subfamily are major players in the development of MDR in Candida albicans. Because several genes coding for ABC proteins exist in the genome of C. albicans but only Cdr1p and Cdr2p have established roles in MDR, it is implicit that the other members of the ABC family also have alternate physiological roles. This study focuses on an ABC transporter of C. albicans, Mlt1p, which is localized in the vacuolar membrane and specifically transports phosphotidylcholine (PC) into the vacuolar lumen. Transcriptional profiling of the mlt1Δ/Δ mutant revealed a down-regulation of the genes involved in endocytosis, oxido-reductase activity, virulence and hyphal development. High-throughput mass spectrometry-based lipidome analysis revealed that the Mlt1p levels impact lipid homeostasis and thus lead to a plethora of physiological perturbations. These include a delay in endocytosis, inefficient sequestering of ROS, defects in hyphal development and attenuated virulence. This study is an emerging example where new and unconventional roles of an ABC transporter are being identified.

Cite as Biochemical Journal (2016) DOI: 10.1042/BCJ20160024

Pleiotropic effects of the vacuolar ABC transporter *MLT1* of *Candida albicans* on cell function and virulence

Nitesh Kumar Khandelwal[1], Philipp Kaemmer[2], Toni M. Förster[2], Ashutosh Singh[3,4], Alix T. Coste[5], David R. Andes[6,7] , Bernhard Hube[2], Dominique Sanglard[5], Neeraj Chauhan[8], Rupinder Kaur[9], Christophe d'Enfert[10], Alok Kumar Mondal[1] and Rajendra Prasad[1,11#]

[1]School of Life Sciences, Jawaharlal Nehru University, New Delhi 110067, India

[2]Department of Microbial Pathogenicity Mechanisms, Leibniz Institute for Natural Product Research and Infection Biology -Hans Knoell Institute Jena (HKI) D-07745 Jena, Germany

[3]Department of Molecular Genetics and Microbiology, Stony Brook University, 145 Life Sciences Building, Stony Brook, NY 11794, USA

[4]Department of Biochemistry, Lucknow University, Lucknow, 226024, Uttar Pradesh, India

[5]Institute of Microbiology, University of Lausanne and University Hospital Center, Lausanne, Switzerland

[6]Department of Medicine, Infectious Diseases, University of Wisconsin, Madison, Wisconsin, USA

[7]Department of Medical Microbiology and Immunology, University of Wisconsin, Madison, Wisconsin, USA

[8]Public Health Research Institute, Department of Microbiology and Molecular Genetics, New Jersey Medical School, Rutgers, The State University of New Jersey, 225 Warren Street, USA

[9]Laboratory of Fungal Pathogenesis, Centre for DNA Fingerprinting and Diagnostics, Hyderabad, Andhra Pradesh, India

[10]Institut Pasteur, Unité Biologie et Pathogénicité Fongiques, Département Génomes et Génétique, Paris, France, INRA, USC2019, Paris, France

[11]Amity Institute of Integrative Sciences and Health, Amity University Haryana, Amity Education Valley Gurgaon-122413, India

Running Title: A vacuolar ABC transporter of *Candida albicans*

 # Corresponding author: Rajendra Prasad,

[1]School of Life Sciences, Jawaharlal Nehru University, New Delhi 110067, India

[11]Amity Institute of Integrative Sciences and Health, Amity University Haryana, Amity Education Valley Gurgaon-122413, India.

E-mail: rp47jnu@gmail.com, rprasad@ggn.amity.edu

Abbreviations:
ABC, ATP-binding cassette; PC, Phosphotidylcholine; MDR, multidrug resistance; MFS, major facilitator; MTX, methotrexate; BSA, bovine serum albumin; NS, Nickel sulphate; DMSO, dimethylsulphoxide; VM, vacuolar membrane; PE, Phosphatidylethanolamine; LPC , lysophosphatidylcholine; LPE, lysophosphatidylethanolamine; PM, Plasma membrane; ROI, Region of Interest.

Key words: *Candida albicans*, *MLT1*, phosphotidylcholine, ABC transporter, Virulence

Abstract
Among the several mechanisms that contribute to multidrug resistance (MDR), the overexpression of drug efflux pumps belonging to the ATP-binding cassette (ABC) superfamily is the most frequent cause of resistance to antifungals. The multidrug transporter proteins Cdr1p and Cdr2p of the ABCG subfamily are major players in the development of MDR in *Candida albicans*. Because several genes coding for ABC proteins exist in the genome of *C. albicans* but only Cdr1p and Cdr2p have established roles in MDR, it is implicit that the other members of the ABC family also have alternate physiological roles. This study focuses on an ABC transporter of *C. albicans*, Mlt1p, which is localized in the vacuolar membrane and specifically transports phosphotidylcholine (PC) into the vacuolar lumen. Transcriptional profiling of the *mlt1*Δ/Δ mutant revealed a down-regulation of the genes involved in endocytosis, oxido-reductase activity, virulence and hyphal development. High-throughput mass spectrometry-based lipidome analysis revealed that the Mlt1p levels impact lipid homeostasis and thus lead to a plethora of physiological perturbations. These include a delay in endocytosis, inefficient sequestering of ROS, defects in hyphal development and attenuated virulence. This study is an emerging example where new and unconventional roles of an ABC transporter are being identified.

Summary
Mlt1 of *C. albicans* transports phosphotidylcholine into the vacuolar lumen. Mlt1 is also required to withstand stresses such as oxidative, ionic and drug stresses. Additionally, its deletion results in altered lipid homeostasis, defects in filamentation or secretary protease activity, culminating in attenuated virulence.

Introduction
Only a few *Candida* species exist in humans commensally, and they may become pathogenic when the microbiota is unbalanced, epithelial barriers are disrupted or the immune system is weakened. Various categories of drugs, such as azoles, polyenes, allylamines, echinocandins, and pyrimidine analogues, are being used to combat *C. albicans* infections. The prolonged use of antifungals increases the probability that *Candida* species develop tolerance not only to the drugs to which they are exposed but also to several other drugs. This phenomenon of multidrug resistance (MDR) is supported by the different strategies adopted by *Candida*, which include target alteration and the overexpression of its gene products. Among the various mechanisms of MDR, enhanced drug extrusion by resistant *Candida* cells represents a prominent strategy. Rapid drug extrusion by resistant *C. albicans* cells is the result of overexpression of the drug efflux

pump-encoding genes *CDR1* and *CDR2*, which belong to the ATP-binding cassette (ABC) and *MDR1* gene families within the major facilitator (MFS) superfamily of transporters [1–4].

The *C. albicans* genome is composed of 26 genes that encode putative ABC superfamily proteins belonging to the ABCB, ABCC, ABCD, ABCF, ABCE, and ABCG major subfamilies. Only two members of this superfamily, Cdr1p and Cdr2p, which belong to the ABCG subfamily, are involved in clinical multidrug resistance. However, the presence of large numbers of proteins in the ABC and MFS superfamilies suggests that they may have distinct physiological roles. These transporter proteins, particularly those belonging to the ABC superfamily, perform diverse functions. The functional diversity of these proteins is reflected by additional roles in absorption, excretion, signal transduction and pathogenesis. For instance, ABC transporters such as ScPdr5 of *S. cerevisiae* or Cdr1p and Cdr2p of *C. albicans*, are phospholipid translocators that maintain membrane asymmetry [5]. The *S. cerevisiae* transporter ScMdl1 is a peptide transporter, whereas ScSte6 exports a-factor pheromone [6,7]. The cryptococcal transporters CnItra1A and CnItra3C not only transport inositol but also affect its virulence [8]. The *Cryptococcus neoformans* ABC transporter gene *CnAFR1* provides resistance to fluconazole and is involved in the delayed phagosomal maturation of phagosomes containing *C. neoformans* cells [9,10] The GDP-mannose transporters CnGmt1 and CnGmt2 of *C. neoformans* are involved in capsule synthesis [11]. The loss of abcB from *Aspergillus fumigatus* invariably elicits increased azole susceptibility and decreased virulence [12]. In *Dictyostelium discoideum,* the ABC transporter AmtA acts as an ammonia transporter and regulates ammonia homeostasis [13]. The ammonium transporter Ump2 of the plant pathogen *Ustilago maydis* also interacts with signaling protein Rho1, which controls polarized growth [14]. The vacuole transporter CgCtr2 of the plant pathogen *Colletotrichum gloeosporioides* is involved in copper transport and impacts its germination and pathogenicity [15].

The present study characterizes *MLT1* of *C. albicans* belonging to the ABCC family. We demonstrate that apart from PC transport into the vacuolar lumen, the *MLT1* levels impact endocytosis, sequestration of ROS, hypha formation and virulence implying its unconventional roles.

Material and Methods

Materials:

Growth media yeast extract-peptone-dextrose (YEPD), serum, luria broth (LB) were purchased from Himedia, (Mumbai, India) YNB was purchased from Difco (Switzerland). $CuSO_4$, $NiSO_4$, KCl, KNO_3, $FeCl_3$, $CaCl_2$, $MgCl_2$, H_2O_2 were obtained from Qualigens. Drug methotrexate (MTX) and chemicals ficoll-400, bovine serum albumin (BSA), NaN_3, creatine phosphate, creatine kinase, quinacrine, 2',7'-dichlorofluorescein diacetate (DCFDA), sucrose, Tris buffer, dimethylsulphoxide (DMSO), MES buffer were purchased from Sigma. *N*-(3-triethylammoniumpropyl)-4-(6-(4-(diethylamino) phenyl) hexatrienyl) pyridinium ibromide (FM4-64) and 1-myristoyl-2-{6-[(7-nitro-2-1,3-benzoxadiazol-4-yl)amino]hexanoyl}-sn-glycero-3-phosphocholine (NBD-PC) were obtained from Life Technologies and Avanti polar lipids (USA), respectively. Anti-His-HRP monoclonal antibody was purchased from Santa Cruz Biotechnology. BCA protein estimation kit was obtained from G Biosciences (USA). The oligonucleotides used in the present study, as listed in table 1 were obtained from Sigma Genosys, India.

Growth media and strains used:
All the yeast strains were grown and maintained in YEPD and YNB media according to experiment requirement. Spot assays were performed in YEPD agar media with or without indicated treatment. Glycerol stock of strains were made in 15% glycerol and maintained at -80°C and freshly revived in YEPD before use. Table 2 lists all the strains used in this study. All plasmids were maintained in the bacterial strain *Escherichia coli* DH5α as a host for the construction and propagation. *E. coli* cells were grown in LB medium containing 0.1 mg/ml ampicillin (Amresco, USA). The list of strains used in the study is given in table 2.

Methods:
MLT1 Plasmid construction:
The *MLT1* gene was amplified using MLT1-PacI FP and MLT1-NotI RP (table 1) primers from the genomic DNA of strain SC5314. The PCR product was inserted into PacI-NotI digested pABC3GFP and pABC3His vectors [16]. Positive clones were confirmed by sequencing. Mutant variants of the WT *MLT1* gene were made by site-directed mutagenesis (SDM) using QuikChange SiteDirected Mutagenesis Kit from Agilent technology, USA as per the manufacturer's instructions [2]. Mutations were introduced into plasmids pABC3-Mlt1-GFP and pABC3-Mlt1-His using the primers MLT1-K710A FP and MLT1-K710A RP (table 1). The mutations were confirmed by sequencing. The mutated plasmids were maintained in *E. coli DH5α*.

Strain construction:
AD-RP strain construction:
A *YBT1* gene deletion cassette along with the KanamaX selection marker gene was amplified from a YBT1 null strain using primers YBT1 null FP and YBT1 null RP (table 1). To construct an AD-RP strain, *S. cerevisiae* strain AD1-8u$^-$ strain was transformed with the PCR product using the lithium acetate method, and transformants were selected on YEPD plates with 25 µg/ml geneticin (Amresco, USA). Genomic DNA was isolated from the putative colonies, and gene deletion was confirmed by using *YBT1* null confirmation primers (table 1).

MLT1 overexpression strains:
To construct strains overexpressing WT (pABC3-Mlt1-GFP and pABC3-Mlt1-His) and mutant variants (pABC3-Mlt1-K710A-GFP and pABC3-Mlt1-K710A-His), plasmids were digested with AscI. The resultant transformation cassettes were used to transform AD-RP cells by a lithium acetate method and selected for uracil prototrophy [16,17].

Bioinformatic analysis:
The topology of Mlt1p was predicted using the online software TOPOCONS, and a cartoon was prepared [18,19]. Phylogenetic analysis was done using the MEGA 6 software.

Spot dilution growth assays:

The susceptibility of strains towards various drugs and chemicals was tested by serial dilution spot assays essentially as described previously [20]. In summary, the strains were grown overnight on YEPD agar plates, and cultures were diluted to OD_{600}= 0.1 in 0.9% saline. From this culture, further 5-fold serial dilutions were made, and 5 µl of cells from each dilution was spotted on to a YEPD agar plate with test chemicals for growth inhibition, and the plates were incubated at 30°C for 48 h. Each experiment was repeated 2-3 times. Representative images are shown.

NBD-PC accumulation assay:

NBD-PC transport study was done in early log phase cells, as described previously [21]. Early log phase cells in YNB medium were incubated with 10 µM NBD-PC for 30 min at 30°C with shaking (200 rpm). Then, the cells were centrifuged at 5000 rpm and washed twice with YNB medium at room temperature. For the visualization of vacuoles, cells were resuspended in 2 ml of YEPD medium to which 20 µM FM4-64 was added and incubated for 1 hr at 30°C under shaking condition. After incubation, the cells were washed twice with ice-cold YNB+NaN_3, and slides were prepared for fluorescence microscopy.

Mlt1p expression and ATPase activity assay:

Purified vacuoles (100 µg) were run on 8% SDS-PAGE gel and transferred to membrane. The membrane was immunodetected with anti-His-HRP monoclonal antibody (Santa Cruz Biotechnology) as described previously [2]. After immunodetection, the membrane was stained with Ponceau S solution and used as a loading control.

For ATPase activity measurement, purified vacuoles (10 µg) were used in an enzymatic assay as described previously [22]. In summary, this assay couples ATP hydrolysis to the oxidation of NADH. The oxidized NADH can be measured as the loss of absorbance at 340 nm. The reaction mixture was incubated at 30°C for 1 h. The vacuole ATPase activity of the AD-RP strain was subtracted from both the WT and mutant version of Mlt1 over-expressing strains to assess ATPase activity specific to Mlt1 protein.

***In vitro* NBD-PC transport assay**:

Vacuoles were purified as described previously using a ficoll density gradient method from *C. albicans* WT(SC5314) and *mlt1Δ/Δ* mutant [23] and kept at 4°C. The NBD-PC uptake assay was performed on freshly prepared vacuolar vesicles at 30°C, as described previously [21]. Uptake was studied in intact vacuoles, which were selected on the basis of limiting membrane staining with FM4-64.

Lipid analysis:

Lipid extraction and analyses was performed using an ESI source on a triple quadrupole mass spectrometer (ESI-MS/MS) (API 4000, Applied Biosystems, Foster City, CA, USA), using methods described earlier [24]. All experiments were performed in triplicate and are represented as the mean ± standard error mean (SEM).

Transcriptome analysis:
C. albicans strains were grown overnight in YEPD in biological duplicates. From primary cultures, cells of OD_{600}=0.2 were inoculated into 15 ml YEPD and allowed to grow for 6 h to reach log phase. The cells were pelleted down at 8000 rpm and washed with DEPC H_2O. RNA was isolated using an RNeasy mini Kit Qiagen, USA as per the manufacturer's instructions. The concentration and purity of RNA samples were estimated using a nano drop spectrophotometer and bioanalyzer. Genotypic Technology Pvt. Ltd., INDIA, performed micro array and data scanning. The threshold value was set to 2-fold to filter out only significantly affected genes. The transcription profile was analyzed using the Go-Slim mapper and was annotated on the basis of biological processes [25].

Microarray accession number:
The microarrays used in the present study along with complete transcriptome data can be accessed from the NCBI Gene Expression Omnibus data base under accession number (GSE70341).

FM4-64 endocytosis and live cell imaging:
C. albicans cells were stained with the lipophilic dye FM4-64. Cells were grown to log phase and incubated in 20 μM FM4-64 dye at static condition at room temperature. An aliquot was withdrawn at different time points to monitor the internalization of the stain.
To monitor time-lapse FM4-64 dye endocytosis in *C. albicans*, early log-phase cells were mixed with 20 μM FM4-64 and fixed on microscopy slides with 2% agarose in YNB. The slide was kept inside a chamber that was maintained at 30°C during time-lapse imaging under a Nikon Eclipse TiE microscope (Japan) equipped with an Andor iXON3 EMCCD camera and controlled using the Andor iQ2.7 software. Image acquisition was started 10 min after the addition of dye and was monitored for a total duration for 3 h with a frequency of 1 image capture /3 min.

Analysis of secretory protease activity:
Extracellular protease activity was assayed on yeast BSA dextrose (YBD) plates [26]. Overnight cultures were washed with phosphate buffered saline (PBS) and set to OD_{600}=1 for each strain. A total of 5 μl of culture was spotted on a YBD plate (BSA agar plate) and incubated at 30°C for 5 days. After 5 days, a plate image was captured by a Biorad ChemiDoc™ XRS+ System, and the diameter of the halo zone surrounding the colony and colony diameter were measured using the quantification tool; halo diameters were normalized to the diameter of the fungal colony, where a value of 1 indicates no halo zone.

Measurement of ROS level:
The oxidant sensitive probe 2',7'-dichlorofluorescein diacetate (DCFDA) was used to measure endogenous reactive oxygen species (ROS) [27]. Cells were set to OD_{600} =0.1 in YEPD medium and incubated for 4 h at 30°C and 200 rpm. Then, a 4 mM final concentration of H_2O_2 was added, and the culture was grown for 2 h. The cells were then divided into two equal parts. One half of the cells was analyzed with a FACSCalibur flow cytometer (Becton Dickinson Immunocytometry Systems, San Jose, CA) at 495 nm excitation and 529 nm emission (filter FL1). A total of 10,000 events were considered. The remaining cells were used to prepare slides and were observed under confocal microscopy with a FITC filter.

Whole blood killing assay:
C. albicans strains SC5314, *mlt1*Δ/Δ and *mlt1*Δ/Δ::*MLT1* were grown overnight in YEPD at 30°C, re-inoculated into fresh YEPD and grown at 30°C to mid-log-phase. The cells were harvested in 1x PBS and diluted into an appropriate concentration. Human whole blood was freshly drawn from healthy volunteers and anticoagulated with recombinant Hirudin (Sarstedt, Nuremberg), which does not influence complement activation. Immediately, yeast cells were added at a concentration of 1 x 10^6 cells per ml whole blood and incubated at 37°C for four hours. After incubation, samples were instantly diluted in ice-cold water and plated on YEPD agar.

Morphogenetic studies:
Hyphae were induced on solid and liquid media as described previously [28]. Briefly, overnight cultures of *C. albicans* strains were washed with PBS and set to $OD_{600=}1$. A total of 10 µl cells were spotted on solid mediums (spider, 10% serum), and the plates were incubated at 37°C for 3 or 6 days. Images were taken with a Nikon SMZ 1500 microscope (Japan). The experiment was repeated at least thrice. Representative images are shown. For a liquid hyphal assay, exponential phase $OD_{600=}1$ cells were diluted to $OD_{600=}0.5$ with different hyphal inducing media and incubated in a 12-well plate at 37°C. Images were captured at the mentioned time points.

Mouse survival assay:
For all mouse experiments, female BALB/c mice (6 weeks old; Charles River France) were housed in ventilated cages with free access to food and water. Yeast strains were grown in individual tubes for 16 h under agitation at 30°C in YEPD medium. Each strain was subsequently diluted 100-fold in YEPD medium and grown overnight under agitation at 30°C. Overnight cultures were washed twice with PBS and resuspended in 5 ml PBS. The concentration of each culture was measured through optical density, and each strain was diluted in PBS to the desired concentration.
For survival experiments with single strain infections, groups of 7 to 10 mice were used. The mice were injected through the lateral tail vein with 250 µl of a cell suspension containing
2 x 10^6 cells/ml. The weight and health of the animals were monitored daily. The post-infection day of natural death or euthanasia of moribund animals was recorded for each mouse. Survival experiments were terminated at 15 days after infection.

Statistical analysis:
Differences in secreted protease activity were compared by one way ANOVA followed by Tukey post hoc test $P<0.001$ represent by *** .Two tailed unpaired Student's t-test was used for comparison of expression of Mlt1 between H_2O_2 treated and untreated cells, where P value = 0.007 is represented by ***. Statistically significant lipid changes were highlighted by the pattern recognition tools like principal component (PCA) using the software XLSTAT (Addinsoft, New York, NY, USA). Statistical significance value of 0.05 was employed using the student *t*-test in lipid species changes.

Ethics Statement:
All survival assay animal experiments were performed at the University Hospital Center of Lausanne with approval through the Institutional Animal Use Committee, Affaires Vétérinaires

du Canton de Vaud, Switzerland (authorization n° 1734.2 and 1734.3), according to decree 18 of the federal law on animal protection. For all mice experiments, female BALB/c mice (6 weeks old; Charles River France) were housed in ventilated cages with free access to food and water.
Human peripheral blood was collected from healthy volunteers with written informed consent. This study was conducted according to the principles expressed in the Declaration of Helsinki. The blood donation protocol and use of blood for this study were approved by the institutional ethics committee of the University Hospital Jena (permission number 2207-01/08).

Results

The topology prediction of Mlt1p suggests that its domain arrangement is similar to that of other MRP proteins. It has a characteristic extra transmembrane domain (TMD) composed of five transmembrane helices (TMHs). Thus, similar to other proteins of the MRP subfamily, Mlt1p has a TMH_5-$(TMD\text{-}NBD)_2$ arrangement as depicted in Fig. 1A. Phylogenetic analysis of Mlt1p with functionally characterized fungal MRP (ABCC) subfamily members revealed its close resemblance to ScBpt1, a vacuolar transporter in *S. cerevisiae* (Fig. 1B). Further, BLASTp analysis with functionally characterized *S. cerevisiae* vacuolar transporters highlights that the Mlt1 protein (Mlt1p) shows close sequence homology with *S. cerevisiae* ScBpt1p (39% identity, 59% similarity), ScYcf1p (40% identity, 46% similarity) and ScYbt1p (30% identity, 48% similarity) (Fig. 1C).

Overexpression of Mlt1p in *S. cerevisiae*

For functional characterization, we used the *S. cerevisiae* AD1-8u$^-$ strain as a heterologous expression system, which lacks seven major ABC transporters including ScYor1p, ScSnq2p, ScPdr5p, ScPdr10p, ScPdr11p, ScYcf1p and ScPdr15p, thus resulting in hypersusceptibility to drugs [29]. This host expression system AD1-8u$^-$ was further derivatized by the deletion of *ScYBT1* (an ion and drug transporter). The resulting strain was designated AD-RP. Because the well characterized vacuolar transporters ScYcf1p and ScYbt1p are involved in drug transport, the deletion of *YBT1* in the AD1-8u$^-$ background provided an overexpression system (AD-RP) with a cleaner background ensuring minimum masking effects due to major ABC transporters of the host. Thus, AD-RP, which is the derivative of AD1-8u$^-$, not only lacks six plasma membrane localized ABC transporters (ScSnq2p, ScPdr5p, ScPdr10p, ScPdr11p, ScYor1p, ScPdr15p) but is also devoid of two major vacuolar transporters (ScYcf1p and ScYbt1*). MLT1* was cloned into the vectors pABC3-GFP and pABC3-His and integrated into strain AD-RP to give strains AD-RP-Mlt1-GFP and AD-RP-Mlt1-HIS expressing Mlt1p from the *PDR5* locus. This strain exhibits a *pdr1-3* allele with a gain-of-function mutation in the transcription factor PDR1, resulting in constitutive high expression of Mlt1p [30]. The localization of overexpressed recombinant Mlt1 protein in AD-RP-Mlt1p-GFP was confirmed by confocal microscopy by employing the vacuolar membrane-specific fluorescent dye FM4-64 and was visualized using a TRITC filter (red fluorescence). The green fluorescence of GFP-tagged Mlt1p distinctly showed a rimmed appearance, specifically on vacuolar membrane (VM), which merged with the red fluorescence of FM4-64. The merged image clearly showed yellow fluorescence, which confirmed the localization of Mlt1-GFP in vacuolar membrane (Fig. 2A upper panel).

Mlt1p levels affect susceptibility to $NiSO_4$ and methotrexate

We performed growth assays with the Mlt1-GFP protein overexpression strain on solid agar media containing different types of ions such as $CuSO_4$, $NiSO_4$, KCl, KNO_3, $FeCl_3$, $CaCl_2$, and $MgCl_2$. There was no growth difference between the Mlt1-GFP protein overexpressing strain (AD-RP-Mlt1p-GFP) and the parental strain (AD-RP) in the majority of the tested conditions (data not shown). However, the overexpression of Mlt1-GFP resulted in resistance to nickel sulphate (NS) compared to the parental AD-RP strain. Fig. 2B depicts that the Mlt1-GFP protein overexpressing strain AD-RP-Mlt1p-GFP could grow on up to 3 mM NS compared with the parental strain AD-RP, which showed no growth at this concentration. Notably, the growth of the strain overexpressing (AD-RP-Mlt1p-GFP) Mlt1-GFP protein remained unaffected in the presence of various other compounds (data not shown). However, it did show increased resistance towards methotrexate (MTX) compared to the parental AD-RP strain (Fig. 2B).

Mlt1p transports NBD-PC into the vacuolar lumen

We examined whether Mlt1p of *C. albicans* could transport phospholipids into vacuoles. For this, we exploited fluorescent NBD tagged phosphatidylcholine (NBD-PC) to monitor phosphatidylcholine (PC) accumulation inside vacuoles. Because fluorescence overlaps between the NBD tag of PC and the GFP tag of Mlt1p, we performed the NBD-PC accumulation assays by using the Mlt1-His tagged overexpression strain (AD-RP-Mlt1p-HIS) and comparing it with the parental AD-RP strain (Fig. 2C). It was evident that the fluorescent NBD-PC specifically accumulated within the vacuolar lumen of AD-RP-Mlt1p-HIS cells, which was further confirmed by the vacuole specific dye FM4-64, whereas the parental strain AD-RP showed no NBD-PC fluorescence in the vacuolar lumen (Fig. 2C).

Deletion of *MLT1* affects NS and MTX susceptibility

As mentioned above, the *S. cerevisiae MLT1* overexpressing strain showed resistance to NS and MTX. We therefore addressed whether the deletion of *MLT1* in *C. albicans* would show the reverse phenotype. Serial dilution assays of *C. albicans* wild type *mlt1*Δ/Δ and *mlt1*Δ/Δ::*MLT1* isolates on NS and MTX revealed that *MLT1* was contributing to NS and MTX resistance. The susceptibility towards both compounds in *mlt1*Δ/Δ was partially reversed in revertant isolates *mlt1*Δ/Δ*::MLT1* (Fig. 3A).

***MLT1* from *C. albicans* is involved in the transport of NBD-PC**

Examination of the NBD-PC accumulation capacity of vacuoles in *C. albicans* strains revealed that wild type *C. albicans* was able to accumulate NBD-PC into the vacuolar lumen (Fig. 3B top panel), however, the *mlt1*Δ/Δ strain did not show any accumulation of NBD-PC, as was evident from the absence of NBD-PC fluorescence within the vacuolar lumen. Indeed, complementation of the null strain with a single allele of *MLT1* could restore NBD-PC accumulation within the vacuolar lumen (Fig. 3B).

NBD-PC transport by Mlt1p into vacuoles is energy dependent

Mlt1p is an ABC transporter, and it is expected that it drives ATP hydrolysis. We checked the energy dependence of NBD-PC accumulation by two independent approaches. In the first instance, we performed the NBD-PC accumulation assay in wild type *C. albicans* (SC5134) cells

treated with sodium azide. As depicted in Fig. 3C, it is clear that following sodium azide treatment, which inhibited ATP hydrolysis, the wild type *C. albicans* cells lost their ability to accumulate NBD-PC into the vacuolar lumen. We also used the AD-RP-Mlt1p-HIS and AD-RP-Mlt1p-GFP strains and changed a well-conserved and critical lysine residue of Walker A of NBD1 (^{704} GKVGSG**K**S ^{711}) to alanine by site-directed mutagenesis. This conserved lysine has been reported to be important for ATP catalysis in many studies [21,31,32], and replacement of it with alanine (K710A) severely reduced ATPase activity (Fig. 2D right panel) and abolished NBD-PC accumulation into vacuoles (Fig. 2C). As expected, the mutant variant (K710A) overexpressing strain also displayed enhanced susceptibility to NS and MTX (Fig. 2B). Confocal images of a strain expressing AD-RP-K710A Mlt1p-GFP confirmed that the K710A mutation did not impact Mlt1p localization. This eliminated the possibility that the inability to accumulate NBD-PC and susceptibility to NS and MTX in the Mlt1p mutant variant could be due to mislocalization of the mutant variant protein (Fig. 2A lower panel). We performed western blotting with vacuoles isolated from the AD-RP-Mlt1-HIS and AD-RP-K710A Mlt1p-HIS strains to show that K710A Mlt1p-His was expressed and localized properly (Fig. 2D left panel).

Mlt1p could transport NBD-PC into the vacuolar lumen *in vitro*

To strengthen the above results that Mlt1p transports NBD-PC and that this process is energy dependent, we performed an *in vitro* NBD-PC transport assay in a cell–free system using isolated vacuoles. For this, we grew *C. albicans* and the *mlt1*Δ/Δ mutant to log phase in YEPD medium and isolated vacuoles by density gradient centrifugation [23]. FM4-64 staining was performed to assess the integrity of the vacuoles. It is evident from Fig. 3D that the isolated vacuoles were intact and could accumulate NBD-PC in presence of 5 mM ATP, whereas this was not the case with vacuoles isolated from the *mlt1*Δ/Δ strain (Fig. 3D lower panel).

Disruption of *MLT1* leads to altered lipid homeostasis

Maintenance of lipid homeostasis by ABC transporters is very important in different organisms. For example, a large number of human genetic disorders related to ABC transporters are due to defects in lipid transport [33]. In the yeast *S. cerevisiae*, MRP family transporters such as ScYbt1 and ScYor1 are involved in PC and PE (phosphatidylethanolamine) translocation, respectively [21,29]. ScYbt1 is able to accumulate PC into the lumen of the vacuole and is involved in phospholipid metabolism in *S. cerevisiae* cells [21]. Mlt1p, which translocates PC into the vacuolar lumen, could also impact lipid homeostasis. We explored this possibility by performing high-throughput mass spectrometry-based lipidome analysis of WT and *mlt1*Δ/Δ strain by ESI–MS/MS.

Our analysis showed that the lipid profile of the *mlt1*Δ/Δ mutant was indeed different from wild type (Fig. 4A and B). The *mlt1*Δ/Δ mutant showed depletion of PC, lysophosphatidylcholine (LPC) and lysophosphatidylethanolamine (LPE) content compared to wild type (Fig. 4A). These data suggest that deletion of *MLT1* alters the overall phospholipid homeostasis of the cell. A closer look at lipid species in the *mlt1*Δ/Δ mutant and wild type using the PCA tool suggested significant modulation of molecular lipid species. The most notable differences were observed among mono-unsaturated (LPE18:1, LPE17:1, PC34:1, PC36:1) and saturated (LPC16:0, LPC15:0, LPE17:0, LPC18:0) lipid species (Fig. 4C).

The *mlt1*Δ/Δ strain transcriptome revealed differential expression of genes related to lipid homeostasis, endocytosis, oxidative stress, hyphal development, biofilm formation and virulence

Because ABC transporters perform various physiological roles, we conducted a genome wide transcriptome analysis of *mlt1*Δ/Δ in comparison with the wild type. The transcription profile was analyzed using CGD Go-slim mapper and was annotated on the basis of biological processes (Fig. S1A and B). The comparative transcriptomic profile revealed that the *mlt1*Δ/Δ strain showed up- and downregulation (≥2-fold) of 33 and 63 genes, respectively (Fig. 5). Notably, the differentially regulated transcripts in the *mlt1*Δ/Δ mutant included genes involved in endocytosis (*ROY1, APS2*), oxidoreductase (*OYE32, AOX2* and *NAD4*), lipid metabolism (*RTA2*), hyphal development (*SSU1, RTA4, DAD48, HGT12* and *FGR46*), biofilm formation, pathogenesis and adherence (*CSH1, TRY6, SIT1* and *HWP1*) as shown in Fig. 5. The expression of some randomly selected genes was validated by semi-quantitative RT-PCR (Fig. S1C).

The *mlt1*Δ/Δ mutant shows a delay in endocytosis

Transcriptome data analysis revealed that gene products involved in endocytosis were down-regulated in the *mlt1*Δ/Δ mutant. We investigated endocytosis in the WT and in the *mlt1*Δ/Δ mutant using FM4-64, a lipophilic dye commonly used to visualize endocytosis by confocal microscopy [34]. The FM4-64 dye stained VM distinctly in WT after 30 min of exposure (Fig. 6A). However, in the *mlt1*Δ/Δ mutant, even after 60 min, most of the dye remained restricted either to the plasma membrane (PM) or between the VM and PM. The delay in FM4-64 endocytosis was confirmed by time-lapse microscopy of WT and *mlt1*Δ/Δ mutant strains. WT cells began to show FM4-64 staining of the vacuolar membrane from 9 min onwards, which became distinctly visible within 30 min. In contrast to WT, the *mlt1*Δ/Δ cells began to show FM4-64 staining of VM only after 90 min of incubation (Fig. S2).

The *mlt1*Δ/Δ mutant displays reduced secretory protease activity

A recent report revealed that vacuolar proteins such as Vph1 could impact the release of secretory proteases in *C. albicans* [22]. We explored whether the Mlt1p vacuolar transporter levels could affect protease secretion. For this, an *in vitro* BSA plate assay for secretory protease activity was performed, wherein the amount of extracellular secreted enzyme activity was quantified by the size of haloes surrounding fungal colonies corresponding to a zone of BSA degradation [26]. As depicted in Fig. 6B, in comparison to wild type, no halo of protein degradation appeared in the *mlt1*Δ/Δ mutant, indicating a deficiency in secretory protease activity or secretion (Fig. 6C). Notably, the defect in secretory protease activity/secretion was not associated with any change in vacuolar lumen pH as measured by quinacrine pH dye (data not shown).

Deletion of *MLT1* affects filamentous growth in *C. albicans*

Our microarray data showed a differential expression of hyphal development related genes (*SSU1, RTA4, DAD48, HGT12,* and *FGR46*) and prompted us to evaluate the hyphal development ability of the *mlt1*Δ/Δ mutant in various hyphal inducing conditions. In liquid hypha inducing medium (serum, spider and RPMI), we performed a time course study of hypha formation. Up to 60 min, it was observed that only few cells from the *mlt1*Δ/Δ mutant showed hypha formation. Only at later time points (120, 180, 240 min) could hyphae be observed,

though their lengths were shorter than those of both wild type and *mlt1*Δ/Δ*::MLT1* cells. Thus, deletion of *MLT1* delayed hypha formation (Fig. 7A, S3B and S3C). Notably, in solid YEPD+10% serum medium, *MLT1* becomes haplo-insufficient, as the single allele null strain *mlt1Δ/MLT1* also showed absence of hypha formation (Fig. 7B). In spider solid medium, the single allele mutant (*mlt1Δ/MLT1*) showed hyphae but of shorter length (Fig. S3A). However, in embedded agar conditions, deletion of *MLT1* did not affect hypha formation (data not shown).
Yeast to hyphal switching can be considered an important virulence factor as mutants that are defective in filament formation show attenuated virulence [35]. The formation of hyphae and their active penetration are involved in host epithelial cell damage [36]. Because the *mlt1Δ/Δ* mutant was defective in hyphal formation, we compared the oral epithelial cell damaging ability of wild type, *mlt1Δ/Δ* and *mlt1*Δ/Δ*::MLT1* cells. However, we did not observe any significant difference in epithelial cell damage between these different cell types (data not shown).
The transcriptome profile and the hyphal formation data indicated that the *mlt1*Δ/Δ mutant could be defective in biofilm formation compared to wild type. Different genes involved in biofilm formation, such as *CSH1, TRY6* and *HWP1*, are differentially expressed in the *mlt1Δ/Δ* mutant compared to wild type. However, a close comparison of the biofilm formation capacity of wild type, *mlt1Δ/Δ* and *mlt1*Δ/Δ*::MLT1* strains in a rat catheter model did not show significant differences (data not shown). This may suggest that the observed down regulation of gene expression in *mlt1Δ/Δ* could be a transient effect not directly associated with *MLT1*. Alternatively, since biofilm formation involves a complex regulatory network, the presence of overlapping genes could mask any detectable phenotype due to altered expression of few genes in *mlt1Δ/Δ* cells.

MLT1 deletion results in hyper-susceptibility to oxidative stress and higher killing by human whole blood-

We observed that some oxidoreductase activity-related genes (*OYE32, AOX2, and NAD4*) are differentially regulated in the *mlt1*Δ/Δ mutant. We checked the survival of the *mlt1*Δ/Δ mutant in the presence of 6 mM H_2O_2 by serial dilution assays. Fig. 8A depicts that in contrast to wild type and *mlt1*Δ/Δ*::MLT1*, the *mlt1*Δ/Δ strain was unable to grow at the tested H_2O_2 concentrations. This finding was well supported by ROS measurements where it was evident from DCFDA (2,7-dichlorofluorescein diacetate), an oxidant-sensitive probe, that the fluorescence of the dye was higher in *mlt1*Δ/Δ cells compared with wild type and *mlt1*Δ/Δ*::MLT1* cells (Fig. 8B). The enhanced level of ROS in *mlt1*Δ/Δ cells was also reflected in fluorescence images that were examined simultaneously in another batch of cells withdrawn from the same suspension. It was apparent that *mlt1*Δ/Δ cells displayed enhanced fluorescence compared to wild type and *mlt1*Δ/Δ*::MLT1* cells (Fig. 8C), thus suggesting that the *MLT1* null strain was not able to sequester ROS efficiently.
Once *C. albicans* enters the host blood stream, neutrophils and macrophage cells play an important role in killing the fungus. ROS generation is one of the key mechanisms in the killing of pathogens by neutrophils. Although the percentage of killing in whole human blood did not show a large difference, there was a noticeable trend of higher killing after four hours in the case of the *mlt1*Δ/Δ mutant (91.1 %) compared with wild type (81.1 %) and *mlt1*Δ/Δ*::MLT1* (83.1 %) strains (Fig. 9A). This may also explain the lower ROS sequestering efficiency of *MLT1* nulls (Fig. 8B and C). However, we did not observe any difference in the killing of wild type versus the *mlt1Δ/Δ* mutant by human primary macrophage cells (data not shown).

To determine the infection capacity of the *mlt1*Δ/Δ mutant, a mouse survival assay was performed. Immunocompetent BALB/c mice were infected with WT (SC5314), *mlt1Δ/Δ* and *mlt1*Δ/Δ*::MLT1* cells. A marked difference in the survival rate of mice infected with WT and *mlt1Δ/Δ* strains was observed. Fully 70% of mice infected with WT *C. albicans* died on day 5, peaking to 100% death at day 8. In contrast to WT, among mice infected with the *mlt1Δ/Δ* mutant only 30% death was recorded at day 5, reaching 100% only after day 11 (Fig. 9B). Notably, mice infected with the revertant *mlt1*Δ/Δ*::MLT1* showed survival closer to the *mlt1Δ/Δ* mutant. This could be because presences of both the *MLT1* alleles are required for maintenance of the virulence trait as both alleles must be retained in order to maintain the proper hyphae formation (Fig.7).

H_2O_2 exposure enhances the level of Mlt1–GFP

Because Mlt1p helps in the survival of *C. albicans* under H_2O_2 stress, we explored whether oxidative stress could also influence the expression of Mlt1p. For this, the fluorescence of GFP in GFP-tagged Mlt1p, which was expressed from its chromosomal locus in *C. albicans*, was quantitated by two methods: by measuring Region of Interest (ROI) intensity using confocal microscopy and by a quantitative estimation of fluorescence using a spectrofluorometer. The ROI mean intensity of the VM was calculated for approximately 40 cells from different fields. Figure 10AE and 8B depict a statistically significant (p=0.007) increase in ROI mean intensity in H_2O_2 treated cells. The Mlt1p-GFP fluorescence quantified by spectrofluorometer further supported the confocal microscopy data, revealing an increase of ~2-fold in the fluorescence intensity following H_2O_2 treatment of *C. albicans* (Fig. 10C).

Discussion

The members belonging to the MRP subfamily of ABC transporters from different organisms have different physiological roles such as transport of PC and PE lipids, ions, bile salt, GS-conjugated compounds, leukotriene C4, glycocholic acid, cyclic nucleotides and ADE pigments; and in vacuole fusion and oxidative stress. [21,29,37–40].Except for the PM localized ScYor1, all the remaining MRP members (ScYbt1, ScYcf1, ScBpt1, ScNft1, and ScVmr1) in *S. cerevisiae,* are localized in the VM and transport different substrates, including ions, bile salt, GS-conjugated compounds and phosphoglycerides [21,41,42]. The commensal pathogenic *C. albicans* has four MRP family members, *MLT1*/orf19.5100, orf19.6478, orf19.6382, and orf19.1783, but none has been assigned any functional role. However, Mlt1 is one of the members of the MRP subfamily in *C. albicans* that is localized in the VM [43]. Our functional analysis in the present study revealed that contrary to an earlier report, which suggested the absence of a *ScYBT1* homologue in *C. albicans* [44], *MLT1* appears to be a functional homologue of this transporter. For instance, similarly to *ScYBT1*, *MLT1* deletion not only results in complete loss of NBD-tagged PC accumulation into the vacuolar lumen, but it also promotes enhanced susceptibility towards NS and MTX.

We observed that *MLT1* levels are critical for withstanding oxidative stress in *C. albicans*. Thus, not only are *mlt1Δ/Δ* cells susceptible to H_2O_2 treatment, but they also have elevated levels of ROS implying lower efficiency of the null strain in its sequestration. Of note, the *ScYCF1* transporter is known to be involved in oxidative stress [39], our data also indicate that *MLT1* has such a role, a notion that is well reinforced by transcriptome data showing differential regulation of oxidative stress related genes (*OYE32, AOX2, NAD4*) in *mlt1Δ/Δ* cells. This result would

imply that *MLT1* is not only able to functionally complement *ScYBT1* but can also partially perform the function of *ScYCF1*. Hence, the vacuolar transporter *MLT1* is capable of performing dual functions, which are otherwise performed by two independent proteins in *S. cerevisiae*. This situation can probably justify the existence of fewer members of the MRP subfamily in the *C. albicans* genome compared to *S. cerevisiae*. Interestingly, the inventory of ABC proteins in the *C. albicans* genome did not identify any homologue of Sc*YBT1*; it did however indicate two putative ORFs, orf19.6478 and orf19.5100/*MLT1*, as *ScYCF1* homologues. Although the former remains uncharacterized, we now report that part of the function of *S. cerevisiae ScYCF1* is performed by *MLT1*. Together, the data from the present and previous studies rule out the existence of real homologues of *ScYBT1* and *ScYCF1* in *C. albicans*, which apparently is taken over by *MLT1* in parts.

Further functional analysis revealed that *MLT1* levels impact cellular endocytosis. For instance, as revealed by time-lapse confocal microscopy, *mlt1Δ/Δ* cells displayed a significant delay in endocytosis (Fig. 6A and S2). The involvement of an ABC transporter in endocytosis appears to be a novel function, but it is not surprising because in different organisms several members of the ABC family have diverse non-transport functions such as in metabolism, germination, pathogenicity, biofilm architecture, polarized growth, capsule synthesis and oxidative stress [8,11,12,15,39,45–48]. Notably, hyphal development in *C. albicans* is already known to be linked to endocytosis with proteins such as Vrp1, Vps1, Vph1, Pep12, Rvs161, and Rvs167 affecting endocytosis and hyphal development [22,49–53].

The behavior of the *mlt1Δ/Δ* mutant with regards to hyphal development could also explain an earlier study wherein an Mlt1-GFP fusion protein was used to study the effect of the RAB GTPase on Golgi-to-vacuole trafficking. It was reported that *vps21Δ/Δ* (Vacuolar Protein Sorting Rab GTPase) cells of *C. albicans* showed defective hyphal formation on agar medium, and this phenotype was enhanced when another GTPase (*YPT52*) was also deleted in the *vps21Δ/Δ* background. However, the deletion of *YPT52* alone in the wild type did not impact hyphal formation [54]. Interestingly in the double knockout (*vps21Δ/Δ*, *ypt52Δ/Δ*), a significant amount of Mlt1p was mis-localized. Considering our observations that deletion of even a single allele of *MLT1* (*mlt1Δ/MLT1*) can lead to a defect in hyphal development, it is thus plausible that the potentiation of hyphal defects by *YPT52* deletion in the *vps21Δ/Δ* null background could have been caused by Mlt1p mis-localization. Interestingly, the *mlt1Δ/Δ* mutant shows a delay in endocytosis and in parallel differential expression of hyphal development related genes. Additionally, the *mlt1Δ/Δ* mutant showed attenuated virulence in an immunocompetent mouse model. Thus, our results also support the well-established correlation between endocytosis, hyphal development and virulence.

Generally, phenotypes such as altered vesicle trafficking, oxidative stress and attenuated virulence are associated with defects in ergosterol biosynthesis in *C. albicans* [55–58]. Additionally, these phenotypes are also mimicked in vacuolar endocytosis mutants [22,49–51,53]. However, in the case of the *mlt1*Δ/Δ mutant, its high ergosterol content suggests that these phenotypes might be independent of the ergosterol pathway (table S1). High ergosterol content could rather be a compensatory change. Interestingly, this consideration emphasizes further that the role of Mlt1 is more attributable to PC transport into the vacuolar lumen.

In conclusion, Mlt1 transports PC into the vacuolar lumen, and it impacts lipid homeostasis, thus leading to delayed endocytosis, defects in hyphae and biofilm, susceptibility to drugs, protease activity/secretion, survival of oxidative stress and killing by whole blood, together culminating in

attenuated virulence (Fig. 11). This study, not only supports the well-known role of ABC transporters in MDR, but it also provides strong evidence in support of multiple functional roles of a member of the ABC transporter superfamily in *C. albicans*.

Acknowledgement:
We acknowledge Dr. Gerwald A Kohler for providing *Candida albicans* Mlt1 mutant strains. We acknowledge Advance Instrumentation Research Facility (AIRF), JNU for providing instrumental support and Mr. Ashok Kumar Sahu and Ms. Tripti Panwar for confocal microscopy and live cell imaging. We are thankful to Dr. K. Natarajan for providing *S.cerevisiae YBT1* null strain. We also thank Mr. Kaushal Kumar Mahto for helping with lipid preparation and Ms. Meghna Gupta for helping in data representation. The help of Dr. Sanjiveeni Dhamgaye, Dr. Peer Abdul Haseeb Shah and Mr. Atanu Banerjee for discussion during work is highly appreciated. N.K.K acknowledges, University Grants Commission, India for a senior research fellowship award. Financial Support from Indo-Swiss Research grant (ISJRP grant No. 122 917) to DS and RP, for supporting N.K.K.'s visit to CHUV, Lausanne is acknowledged.

Conflict of interest: The authors declare no conflict of interest.

Funding:
The work has been supported, in parts by grants to RP from the Department of Biotechnology: DBT No.BT/01/CEIB/10/III/02; DBT No.BT/PR7392/MED/29/652/2012 and DBT No.BT/PR14879/BRB10/885/2010.

Author Contributions:
N.K.K, A.S, B.H, D.R.A, D.S, R. P designed the experiments; N.K.K, P.K, T.F, A.T.C, D.R.A performed the experiments; N.K.K, A.S, B.H, D.R.A, D.S, A.K.M, N.C, R.K, C.dE, R.P analysed the data with inputs from the other authors; B.H, D.R.A, D.S, R.P contributed reagents/materials; N.K.K, A.S, B.H, D.S, A.K.M, R.P wrote the paper with input from the other authors. All authors read and approved the final manuscript.

References:

1 White, T. C., Holleman, S., Dy, F., Laurence, F., Stevens, D. a and Mirels, L. F. (2002) Resistance mechanisms in clinical isolates of Candida albicans. Antimicrob. Agents Chemother. **46**, 1704–1713.

2 Shukla, S., Saini, P., Jha, S., Ambudkar, V., Prasad, R. and Ambudkar, S. V. (2003) Functional Characterization of Candida albicans ABC Transporter Cdr1p Functional Characterization of Candida albicans ABC Transporter Cdr1p **2**, 1361–1375.

3 Liu, T. T., Znaidi, S., Barker, K. S., Xu, L., Homayouni, R., Saidane, S., Morschhäuser, J., Nantel, A., Raymond, M. and Rogers, P. D. (2007) Genome-wide expression and location analyses of the Candida albicans Tac1p regulon. Eukaryot. Cell **6**, 2122–2138.

4 Sanglard, D., Ischer, F., Monod, M. and Bille, J. (1997) Cloning of Candida albicans genes conferring resistance to azole antifungal agents: Characterization of CDR2, a new multidrug ABC transporter gene. Microbiology **143**, 405–416.
5 Smriti, Krishnamurthy, S., Dixit, B. L., Gupta, C. M., Milewski, S. and Prasad, R. (2002) ABC transporters CdrLp, Cdr2p and Cdr3p of a human pathogen candida albicans are general phospholipid translocators. Yeast **19**, 303–318.
6 Young, L., Leonhard, K., Tatsuta, T., Trowsdale, J. and Langer, T. (2001) Role of the ABC transporter Mdl1 in peptide export from mitochondria. Science **291**, 2135–2138.
7 Ketchum, C. J., Schmidt, W. K., Rajendrakumar, G. V., Michaelis, S. and Maloney, P. C. (2001) The Yeast a-factor Transporter Ste6p, a Member of the ABC Superfamily, Couples ATP Hydrolysis to Pheromone Export. J. Biol. Chem. **276**, 29007–29011.
8 Wang, Y., Liu, T. B., Delmas, G., Park, S., Perlin, D. and Xue, C. (2011) Two major inositol transporters and their role in cryptococcal virulence. Eukaryot. Cell **10**, 618–628.
9 Sanguinetti, M., Posteraro, B., La Sorda, M., Torelli, R., Fiori, B., Santangelo, R., Delogu, G. and Fadda, G. (2006) Role of AFR1, an ABC transporter-encoding gene, in the in vivo response to fluconazole and virulence of Cryptococcus neoformans. Infect. Immun. **74**, 1352–1359.
10 Orsi, C. F., Colombari, B., Ardizzoni, A., Peppoloni, S., Neglia, R., Posteraro, B., Morace, G., Fadda, G. and Blasi, E. (2009) The ABC transporter-encoding gene AFR1 affects the resistance of Cryptococcus neoformans to microglia-mediated antifungal activity by delaying phagosomal maturation. FEMS Yeast Res. **9**, 301–310.
11 Cottrell, T. R., Griffith, C. L., Liu, H., Nenninger, A. a. and Doering, T. L. (2007) The pathogenic fungus Cryptococcus neoformans expresses two functional GDP-mannose transporters with distinct expression patterns and roles in capsule synthesis. Eukaryot. Cell **6**, 776–785.
12 Paul, S., Diekema, D. and Moye-Rowley, W. S. (2013) Contributions of Aspergillus fumigatus ATP-binding cassette transporter proteins to drug resistance and virulence. Eukaryot. Cell **12**, 1619–1628.
13 Yoshino, R., Morio, T., Yamada, Y., Kuwayama, H., Sameshima, M., Tanaka, Y., Sesaki, H. and Iijima, M. (2007) Regulation of ammonia homeostasis by the ammonium transporter AmtA in Dictyostelium discoideum. Eukaryot. Cell.
14 Paul, J. a., Barati, M. T., Cooper, M. and Perlin, M. H. (2014) Physical and Genetic Interaction between Ammonium Transporters and the Signaling Protein Rho1 in the Plant Pathogen Ustilago maydis. Eukaryot. Cell **13**, 1328–1336.
15 Barhoom, S., Kupiec, M., Zhao, X., Xu, J. R. and Sharon, A. (2008) Functional characterization of CgCTR2, a putative vacuole copper transporter that is involved in germination and pathogenicity in Colletotrichum gloeosporioides. Eukaryot. Cell **7**, 1098–1108.
16 Lamping, E., Monk, B. C., Niimi, K., Holmes, A. R., Tsao, S., Tanabe, K., Niimi, M., Uehara, Y. and Cannon, R. D. (2007) Characterization of three classes of membrane proteins involved in fungal azole resistance by functional hyperexpression in Saccharomyces cerevisiae. Eukaryot. Cell **6**, 1150–1165.
17 Gietzt, R. D., Schiestls, R. H., Willems, A. R. and Woods, R. a. (1995) Studies on the Transformation of Intact Yeast Cells by the LiAc / SS-DNA / PEG Procedure **11**, 355–360.

18 Bernsel, A., Viklund, H., Hennerdal, A. and Elofsson, A. (2009) TOPCONS: Consensus prediction of membrane protein topology. Nucleic Acids Res. **37**, 465–468.
19 Tsirigos, K. D., Peters, C., Shu, N., Kall, L. and Elofsson, a. (2015) The TOPCONS web server for consensus prediction of membrane protein topology and signal peptides. Nucleic Acids Res. 1–7.
20 Mukhopadhyay, K., Kohli, A. and Prasad, R. (2002) Drug Susceptibilities of Yeast Cells Are Affected by Membrane Lipid Composition Drug Susceptibilities of Yeast Cells Are Affected by Membrane Lipid Composition.
21 Gulshan, K. and Moye-Rowley, W. S. (2011) Vacuolar import of phosphatidylcholine requires the ATP-Binding cassette transporter ybt1. Traffic **12**, 1257–1268.
22 Raines, S. M., Rane, H. S., Bernardo, S. M., Binder, J. L., Lee, S. a. and Parra, K. J. (2013) Deletion of vacuolar proton-translocating ATPase Voa isoforms clarifies the role of vacuolar pH as a determinant of virulence-associated traits in Candida albicans. J. Biol. Chem. **288**, 6190–6201.
23 Bankaitis, V. a, Johnson, L. M. and Emr, S. D. (1986) Isolation of yeast mutants defective in protein targeting to the vacuole. Proc. Natl. Acad. Sci. U. S. A. **83**, 9075–9079.
24 Mahto, K. K., Singh, A., Khandelwal, N. K., Bhardwaj, N., Jha, J. and Prasad, R. (2014) An Assessment of Growth Media Enrichment on Lipid Metabolome and the Concurrent Phenotypic Properties of Candida albicans. PLoS One **9**, e113664.
25 Boyle, E. I., Weng, S., Gollub, J., Jin, H., Botstein, D., Cherry, J. M. and Sherlock, G. (2004) GO::TermFinder - Open source software for accessing Gene Ontology information and finding significantly enriched Gene Ontology terms associated with a list of genes. Bioinformatics **20**, 3710–3715.
26 K.Ross, I. (1990) The Secreted aspartate proteinase of Candida albicans:physiology of secretion and virulence of aproteinase-deficient mutant 687–694.
27 Dhamgaye, S., Devaux, F., Vandeputte, P., Khandelwal, N. K., Sanglard, D., Mukhopadhyay, G. and Prasad, R. (2014) Molecular Mechanisms of Action of Herbal Antifungal Alkaloid Berberine, in Candida albicans. PLoS One **9**, e104554.
28 Prasad, T., Saini, P., Gaur, N. A., Ram, a, Khan, L. A., Haq, Q. M. R. and Vishwakarma, R. a. (2005) Functional Analysis of Ca IPT1 , a Sphingolipid Biosynthetic Gene Involved in Multidrug Resistance and Morphogenesis of Candida albicans Functional Analysis of CaIPT1 , a Sphingolipid Biosynthetic Gene Involved in Multidrug Resistance and Morphogenesis of **49**, 3442–3452.
29 Decottignies, A., Grant, A. M., Nichols, J. W., De Wet, H., McIntosh, D. B. and Goffeau, A. (1998) ATPase and multidrug transport activities of the overexpressed yeast ABC protein Yor1p. J. Biol. Chem. **273**, 12612–12622.
30 Nakamura, K., Niimi, M., Niimi, K., Ann, R., Yates, J. E., Decottignies, A., Brian, C., Goffeau, A., Cannon, R. D. and Holmes, a N. N. R. (2001) Functional Expression of Candida albicans Drug Efflux Pump Cdr1p in a Saccharomyces cerevisiae Strain Deficient in Membrane Transporters Functional Expression of Candida albicans Drug Efflux Pump Cdr1p in a Saccharomyces cerevisiae Strain Deficient in Mem **45**, 3366–3374.
31 Frelet, A. and Klein, M. (2006) Insight in eukaryotic ABC transporter function by mutation analysis **580**, 1064–1084.
32 Ren, X.-Q., Furukawa, T., Haraguchi, M., Sumizawa, T., Aoki, S., Kobayashi, M. and

Akiyama, S. (2004) Function of the ABC signature sequences in the human multidrug resistance protein 1. Mol. Pharmacol. **65**, 1536–1542.
33 Paulusma, C. C. and Oude Elferink, R. P. J. (2006) Diseases of intramembranous lipid transport. FEBS Lett. **580**, 5500–5509.
34 Vida, T. a. and Emr, S. D. (1995) A new vital stain for visualizing vacuolar membrane dynamics and endocytosis in yeast. J. Cell Biol. **128**, 779–792.
35 Lo, H., Ko, J. R., Didomenico, B., Loebenberg, D., Cacciapuoti, A. and Fink, G. R. (1997) Nonfilamentous C . albicans Mutants Are Avirulent. Cell **90**, 939–949.
36 Wilson, D., Haedicke, K., Dalle, F., Hube, B. and Wa, B. (2011) From Attachment to Damage : Defined Genes of Candida albicans Mediate Adhesion , Invasion and Damage during Interaction with Oral Epithelial Cells **6**.
37 Klein, M., Mamnun, Y. M., Eggmann, T., Schüller, C., Wolfger, H., Martinoia, E. and Kuchler, K. (2002) The ATP-binding cassette (ABC) transporter Bpt1p mediates vacuolar sequestration of glutathione conjugates in yeast. FEBS Lett. **520**, 63–67.
38 Kruh, G. D. and Belinsky, M. G. (2003) The MRP family of drug efflux pumps. Oncogene **22**, 7537–7552.
39 Lee, M. E., Singh, K., Snider, J., Shenoy, A., Paumi, C. M., Stagljar, I. and Park, H. O. (2011) The Rho1 GTPase acts together with a vacuolar glutathione S-conjugate transporter to protect yeast cells from oxidative stress. Genetics **188**, 859–870.
40 Sasser, T. L., Lawrence, G., Karunakaran, S., Brown, C. and Fratti, R. a. (2013) The yeast ATP-binding cassette (ABC) transporter Ycf1p enhances the recruitment of the soluble SNARE Vam7p to vacuoles for efficient membrane fusion. J. Biol. Chem. **288**, 18300–18310.
41 Li, Z. S., Szczypka, M., Lu, Y. P., Thiele, D. J. and Rea, P. a. (1996) The yeast cadmium factor protein (YCF1) is a vacuolar glutathione S-conjugate pump. J. Biol. Chem. **271**, 6509–6517.
42 Sharma, K. G., Mason, D. L., Liu, G., Rea, P. a., Bachhawat, A. K. and Michaelis, S. (2002) Localization, regulation, and substrate transport properties of Bpt1p, a Saccharomyces cerevisiae MRP-type ABC transporter. Eukaryot. Cell **1**, 391–400.
43 Theiss, S., Kretschmar, M., Nichterlein, T., Hof, H., Agabian, N., Hacker, J. and Köhler, G. a. (2002) Functional analysis of a vacuolar ABC transporter in wild-type Candida albicans reveals its involvement in virulence. Mol. Microbiol. **43**, 571–584.
44 Kovalchuk, A. and Driessen, A. J. M. (2010) Phylogenetic analysis of fungal ABC transporters. BMC Genomics **11**, 177.
45 Mayer, F. L., Wilson, D., Jacobsen, I. D., Miramón, P., Große, K. and Hube, B. (2012) The novel Candida albicans transporter Dur31 is a multi-stage pathogenicity factor. PLoS Pathog. **8**.
46 Albicans, C. and Bishop, A. C. (2013) TRANSPORT AND METABOLISM OF GLYCEROPHOSPHODIESTERS BY Submitted to the Bayer School of Natural and Environmental Sciences the degree of Doctor of Philosophy.
47 Shah, A. H., Singh, A., Dhamgaye, S., Chauhan, N., Vandeputte, P., Suneetha, K. J., Kaur, R., Mukherjee, P. K., Chandra, J., Ghannoum, M. a, et al. (2014) Novel role of a family of major facilitator transporters in biofilm development and virulence of Candida albicans. Biochem. J. **460**, 223–35.
48 Tran, P. N., Brown, S. H. J., Mitchell, T. W., Matuschewski, K., McMillan, P. J., Kirk, K.,

Dixon, M. W. a. and Maier, A. G. (2014) A female gametocyte-specific ABC transporter plays a role in lipid metabolism in the malaria parasite. Nat. Commun., Nature Publishing Group **5**, 4773.

49 Barelle, C. J., Richard, M. L., Gaillardin, C., Gow, N. a R. and Brown, a. J. P. (2006) Candida albicans VAC8 is required for vacuolar inheritance and normal hyphal branching. Eukaryot. Cell **5**, 359–367.

50 Cornet, M., Bidard, F., Schwarz, P., Costa, D., Blanchin-roland, S. and Dromer, F. (2005) Deletions of Endocytic Components VPS28 and VPS32 Affect Growth at Alkaline pH and Virulence through both RIM101 Pathways in Candida albicans Deletions of Endocytic Components VPS28 and VPS32 Affect Growth at Alkaline pH and Virulence through both RIM101 **73**, 7977–7987.

51 Bernardo, S. M., Khalique, Z., Kot, J., Jones, J. K. and Lee, S. a. (2008) Candida albicans VPS1 contributes to protease secretion, filamentation, and biofilm formation. Fungal Genet. Biol. **45**, 861–877.

52 Douglas, L. M., Martin, S. W. and Konopka, J. B. (2009) BAR domain proteins Rvs161 and Rvs167 contribute to Candida albicans endocytosis, morphogenesis, and virulence. Infect. Immun. **77**, 4150–4160.

53 Palanisamy, S. K. a, Ramirez, M. a., Lorenz, M. and Lee, S. a. (2010) Candida albicans PEP12 is required for biofilm integrity and in Vivo virulence. Eukaryot. Cell **9**, 266–277.

54 Johnston, D. a., Tapia, A. L., Eberle, K. E. and Palmer, G. E. (2013) Three prevacuolar compartment Rab GTPases impact Candida albicans hyphal growth. Eukaryot. Cell **12**, 1039–1050.

55 Mukherjee, P. K., Chandra, J., Kuhn, D. M. and Ghannoum, M. a. (2003) Mechanism of fluconazole resistance in Candida albicans biofilms: Phase-specific role of efflux pumps and membrane sterols. Infect. Immun. **71**, 4333–4340.

56 Thorpe, G. W., Fong, C. S., Alic, N., Higgins, V. J. and Dawes, I. W. (2004) Cells have distinct mechanisms to maintain protection against different reactive oxygen species: oxidative-stress-response genes. Proc. Natl. Acad. Sci. U. S. A. **101**, 6564–6569.

57 Zhang, Y. Q., Gamarra, S., Garcia-Effron, G., Park, S., Perlin, D. S. and Rao, R. (2010) Requirement for ergosterol in V-ATPase function underlies antifungal activity of azole drugs. PLoS Pathog. **6**.

58 Landolfo, S., Zara, G., Zara, S., Budroni, M., Ciani, M. and Mannazzu, I. (2010) Oleic acid and ergosterol supplementation mitigates oxidative stress in wine strains of Saccharomyces cerevisiae. Int. J. Food Microbiol., Elsevier B.V. **141**, 229–235.

59 Mullaney, E. J., Hamer, J. E., Roberti, K. a, Yelton, M. M. and Timberlake, W. E. (1985) Mol Gen Genet. Prim. Struct. trpC gene from Aspergillus nidulans.

Figure Legends

Figure 1 Bioinformatic analysis of Mlt1 transporter of *C. albicans*. (A) Pictorial representation of the putative topology of Mlt1p as predicted by TOPCONS software showing typical domain arrangement of MRP proteins including a regulatory domain (R-domain) in transmembrane-12 (TM12). (B) Phylogenetic analysis of *C. albicans* Mlt1p with yeast ABCC/MRP transporters of known functions. The analysis shows that the Mlt1p transporter is closest to Bpt1transporter of *S.*

cerevisiae. Phylogenetic tree was generated using MEGA 6 software. Value at nodes represents bootstrap values signifying confidence levels**.** (C) BLASTp analysis of Mlt1p and *S.cerevisiae* vacuolar MRP transporters (ScYbt1, ScBpt1 and ScYcf1) of known functions.

Figure 2 Expression, localization and characterization of WT Mlt1p and its mutant variant in a heterologous overexpressing strain. (A) Fluorescence imaging by confocal microscope (right panel) showing vacuolar membrane (VM) localization of Mlt1p-GFP and Mlt1p-K710A-GFP proteins with corresponding differential interference contrast (DIC) images, FM4-64 staining and merged images. Scale bar represents 10 μm. (B) A comparison by spot dilution assays of susceptibilities of over expressing strains AD-RP-Mlt1p-GFP, AD-RP-K710A Mlt1p -GFP with parental AD-RP strain. A 5-fold serial dilution of each strain was spotted on to NiSO4 and methotrexate (MTX) at the indicated concentrations, in YEPD agar plates and grown for 48 h at 30°C. (C) NBD-PC accumulates in vacuolar lumen of wild type Mlt1p-His overexpressing strain (AD-RP-Mlt1p-HIS). Overexpression strains AD-RP-Mlt1p-HIS, AD-RP- K710A Mlt1p-HIS and parental strain AD-RP were grown to mid-log phase and incubated with NBD-PC. After incubation, cells were washed and stained with FM4-64. Samples were prepared for microscopy and photographed using confocal microscope. Scale bar represents 10 μm. (D) Immunoblot (left panel) showing expression of Mlt1p-K710A-His and WT Mlt1p-His proteins. Vacuoles were isolated by ficoll gradient method and equal amounts of proteins (100 μg) were resolved on 8% SDS–PAGE gel and then probed with anti-His antibody. After probing, membrane was stained with ponceau S which is used as a loading control. ATPase activities (right panel) in purified vacuolar vesicles from AD-RP-Mlt1p-HIS and AD-RP-Mlt1p-K710A-HIS strains were measured using an enzyme assay coupled to NADH oxidation at 340 nm. ATP hydrolysis is 60% reduced in Mlt1p-K710A-HIS mutants. Data are mean±s.d. (n = 3).

Figure 3 Mlt1p levels are required to maintain growth in presence of $NiSO_4$, methotrextate and for accumulation of NBD-PC into vacuolar lumen. (A) Comparison of growth by spot dilution assays of *C. albicans* WT (SC5314), *mlt1Δ/Δ* and *mlt1Δ/Δ::MLT1* cells. A 5-fold serial dilution of each strain was spotted on to NiSO4 and MTX at the indicated concentrations, in YEPD agar plates and grown for 48 h at 30°C. (B) Deletion of *MLT1* results in the loss of accumulation of NBD-PC in vacuolar lumen. *C. albicans* WT (SC5314), *mlt1Δ/Δ,* and *mlt1Δ/Δ::MLT1* cells were grown to mid-log phase and incubated with NBD-PC. After incubation cells were washed and stained with FM4-64. Samples were prepared for microscopy and photographed using confocal microscope. Scale bar represents 10 μm. (C) NBD-PC accumulation into vacuolar lumen of *C. albicans* is energy dependent. Azide treatment was given to mid-log phase WT *C. albicans* (SC5314) cells before their incubation with NBD-PC. The cells were photographed using confocal microscope. (D) NBD-PC accumulation into the vacuolar lumen is energy dependent. Vacuoles were isolated from WT and *mlt1Δ/Δ* mutant of *C. albicans* using ficoll gradient ultracentrifuge based method as described in experimental section. Equal amounts (25μg) of purified vacuolar vesicles were then incubated at 30°C for 30 min in buffer containing 10 μM NBD-PC and 10 μM FM4-64. Transport assay was done under two conditions: one in the absence of energy source ATP and another in presence of 5 mM ATP. After Incubation samples were washed with ice-chilled Tris/Sucrose buffer containing 3% fatty acid-free BSA and observed under confocal microscope. In presence of ATP the isolated vacuoles from WT

C. albicans showed NBD-PC accumulation. While, there was no NBD-PC accumulation in the absence of ATP in WT cells and in vacuoles isolated from *mlt1Δ/Δ* mutant.

Figure 4 Deletion of Mlt1 results in altered lipid homeostasis. (A) Lipid profile of *mlt1*Δ/Δ mutant compared to the wild type (WT). The values represent the percentage of total PGL + SL + sterol mass spectral signal. Mean ± s.e.m. are shown (n = 3). **P* < 0.05 (student's t-test). (B) PCA analyses of all lipid species analyzed shows that the three replicates are grouped, WT (red), *mlt1*Δ/Δ mutant (blue); and that there lipid profiles are different. Factors F1 (x-axis) and F2 (y-axis) represent the two most variable principal components. (C) PCA analyses of LPC, LPE, PC and sterols. PCA loading plots (left) represent the contribution of individual species to the sample variability. PCA plots showing grouping of replicates are on right. LPC: lysophosphatidylcholine; PC: phosphatidylcholine; LPE: lysophosphatidylethanolamine; PE: phosphatidylethanolamine; PI: phosphatidylinositol; PS: phosphatidylserine; PA: phosphatidic acid; PG: phosphatidylglycerol; IPC: inositolphosphorylceramide; MIPC: mannosylinositolphosphorylceramide; $M(IP)_2C$: mannosyldiinositolphosphorylceramide.

Figure 5 The comparative trasnscriptomic profile of *mlt1Δ/Δ* mutant.
The genes with ≥ 2-fold change are shown. The intensity of the colour represents the extent of change in the expression values with red for up-regulation and violet for down-regulation as per the given scale. The affected genes involved in endocytosis, oxido reductase, lipid metabolism, hyphal development, biofilm formation, pathogenesis and adherence are labeled with colour box. The different colour box represents different gene categories.

Figure 6 *mlt1Δ/Δ* mutant shows delay in endocytosis of lipophilic dye FM4-64and loss of secreted protease activity. (A) Endocytosis process was studied using FM4-64 dye in WT and *mlt1Δ/Δ* mutant of *C. albicans*. Log-phase cells were incubated in 20 μM FM4-64 for time point of 30, 40, 50, 60 mins at static condition and monitored for internalization of the stain. In case of WT, most of the dye was internalized by endocytosis process and can be seen at vacuolar membrane while in *mlt1Δ/Δ* mutant, the dye remained restricted either at plasma membrane or between vacuolar and plasma membrane. (B) Overnight cultures were spotted onto BSA agar plates and grown at 30°C for 5 days. The zone of BSA degradation surrounding the fungal colony represents the secreted protease activity. Representative images are shown for WT, *mlt1Δ/Δ* and *mlt1Δ/Δ :MLT1* strains. (C) The quantification of secreted protease activity was done by measuring the diameter of the degradation halo surrounding the fungal colony and was normalized to the diameter of the colony itself; thus a ratio of 1 indicates a lack of detectable halo. Data are mean ± s.e.m. Halo size is shown as the average for n=7 replicates. P<0.001 represent as *** WT V/S *mlt1Δ/Δ* and *mlt1Δ/Δ* V/S *mlt1Δ/Δ :MLT1* strains calculated by one way ANOVA followed by Tukey post hoc test.

Figure 7 Deletion of *MLT1* effects hyphal growth in *C. albicans*. (A) *C. albicans* WT (SC5314), *mlt1Δ/Δ* and *mlt1Δ/Δ::MLT1* were incubated in liquid YEPD medium containing 10% serum at 37°C and images were captured after 60 mins,120 min,180 min and 240 min incubation time point. (B) *MLT1* mutant becomes haplo-insufficient at solid hyphal inducing media. *C. albicans* WT (SC5314), *MLT1/mlt1Δ* , *mlt1Δ/Δ, mlt1Δ/Δ::MLT1* strains were spotted on YEPD containing 10% serum agar plate and incubated at 37°C for 6 days. Scale bar represents 100 μm.

Figure 8 *MLT1* mutant is susceptible to oxidative stress by H_2O_2 and show low ROS sequestration.
(A) Comparison of growth by spot dilution assays of *C. albicans* WT (SC5314), *mlt1Δ/Δ* and *mlt1Δ/Δ::MLT1* cells. A 5-fold serial dilution of each strain was spotted on to 6 mM H_2O_2 containing YEPD agar and YEPD control and grown for 48 h at 30°C **(B)** Histograms (n=10,000 cells for each sample) of measurement of ROS generation by FACS analysis using DCFDA in WT (SC5314), *mlt1Δ/Δ* and *mlt1Δ/Δ::MLT1* cells after treatment with sub-lethal concentration 4 mM H_2O_2 for 2 h. **(C)** Confocal images of aliquoted samples used in FACS to measure ROS by DCFDA in WT (SC5314), *mlt1Δ/Δ* and *mlt1Δ/Δ::MLT1*.

Figure 9 *mlt1Δ/ Δ* mutant is shows attenuation in virulence. (A) Killing assay for *C. albicans* WT (SC5314), *mlt1Δ/Δ* and *mlt1Δ/Δ::MLT1* cells in human whole blood after four hours showing higher tendency of killing the *mlt1Δ/Δ* mutant. (B) Survival curve of mice infected with *mlt1Δ/Δ* mutant shows attenuation in virulence as the mice infected with mutant strains survived up to 11 days post-infection compared with the WT *C. albicans* strains where all the mice succumbed to infection within 8 days. Virulence was partially restored when a single copy of *MLT1* gene was added back to mutants.

Figure 10 H_2O_2 treatment induces the expression of Mlt1–GFP. (A) Log phase cells of *C. albicans* expressing GFP tagged Mlt1 protein from its chromosomal locus was further grown for 2 h with or without 4 mM H_2O_2. The cells were then washed with PBS and observed under fluorescent microscope. Representative images are shown. (B) Region of Interest (ROI) intensity measured using NIS elements AR are plotted. Data are mean ± s.e.m. (n=37 for untreated and n=40 for treated sample).Two tailed unpaired t test was used P=0.007 represent as ***. (C) Equal no. of cells (OD_{600} =1) were set in PBS buffer in aliquoted samples treated for 2 h with or without 4 mM H_2O_2 and quantitation of Mlt1p-GFP fluorescence was measured by spectrofluorometer. The data are shown as means ± s.d. significant difference (P<0.0004 represent as ***) between mutant and wild-type strains as measured by unpaired t test.

Figure 11 Proposed model for vacuolar Mlt1 transporter function and its roles in different phenotypes. Mlt1p which is localized to vacuolar membrane transports PC analogue NBD-PC in to vacuolar lumen in an energy dependent manner and maintains lipid homeostasis. Thus *MLT1* deletion may lead to defect in endocytosis and virulence. Deletion of *MLT1* also negatively affects various virulence related traits like hyphae formation, secretory protease activity/ secretion, sensitivity to oxidative stress. Thus all these phenotypes show their cumulative effect to attenuated virulence in the *mlt1Δ/Δ* mutant.

Tables

Table 1: List of primers used in the study.

Primer name	Primer sequence
YBT1 null FP	5’ GCAGCTAATATAAACAAGTGATC 3’
YBT1 null RP	5’ CGACTGGAATATTGAAGTTAACGG 3’
YBT1 del con FP	5’CTAAAGAAAAAGCCACTCAAG3’
YBT1 del con RP	5’CTTCGCGCCGTGCGGCCATC3’
MLT1-PacI FP	5’CGCGATTAATTAAATGAATGAACTGAATAGAGAACTTATC3’
MLT1-NotI RP	5’CGCGAGCGGCCGCAATCTATGTATCCACCTTCTTTGGC3’
MLT1-K710A FP	5’AAAGTTGGAAGTGGGGCATCTACTTTGATTAAG3’
MLT1-K710A RP	5’CTTAATCAAAGTAGATGCCCCACTTCCAACTTT3’
Hgt12 FP	5’GTTGTTATGGCTGTCTCCCAA3’
Hgt12 RP	5’CCACAAATAGCCCAACAAAGA3’
SIT1 FP	5’AATCCATTGGGGTTGAAAAAG3’
SIT1 RP	5’ACATCCGACAATCTGGCATAG3’
NAD4 FP	5’TGTATCTCCGCAGGTATAATGG3’
NAD4 RP	5’GCTAATAGCATTGAACCAGCAA3’
FGR46 FP	5’TGAACAAGGGCAGAAAGAAGA3’
FGR46 RP	5’GCAATCAGACGCAGTTGAAAT3’
AOX2 FP	5’CCTTCGTCATTTGCATTCATT3’
AOX2 RP	5’AATTTCCCAGGAACAGCAAGT3’
ROY1 FP	5’CAACTACTACCGTCGTTGGGA3’
ROY1 RP	5’ACTCGTCCAAATCTCCAAGGT3’
RTA4 FP	5’TTCTATAGCGGCTCAACGGTA3’

RTA4 RP	5'TGGTCGACCTCGTAAATCTTG3'
RTA2 FP RTA2 RP	5'CAGTTTTGAAGCCAATGTGGT3' 5'TTATCGAACGTCGACCATAGG3'
CSH1 FP CSH1 RP	5'GTCAAAGACGACGCAGAAGAC3' 5'TTTGCAACTCAACAAATTCCC3'
OYE32 FP OYE32 RP	5'CCAATTGTCGATTACGCTCAT3' 5'TTCTAGCAGCAGCACCAAAAT3'
ACT1 FP ACT1 RP	5'GGGTAGGGTGGGAAAACTTCA3' 5'TTGAAACCACTGCCGACAGA3'

Table 2: List of strains used in the study.

Strain	Genotype/Description	Source/Reference
WT(SC5314)	Wild type strain	[59]
mlt1Δ/MLT1 (ST13–9)	ST13 derivative, Δ*mlt1–1::his*G/*MLT1*	[43]
*mlt1*Δ/Δ (ST13–63)	ST13–12 derivative, Δ*mlt1–1::his*G/Δ*mlt1–2::his*G	[43]
*mlt1*Δ/Δ::*MLT1* (ST13-K2)	ST13–63 derivative, Δ*mlt1–1::his*G/*MLT1-MPA^R*	[43]
C4GFP	CAI4 derivative, *MLT1/MLT1::GFP-URA3*	[43]
AD-RP	AD1-8U$^-$ derivative (*Mata,pdr1-3,ura3 his1, Δyor1::hisG, Δsnq2::hisG, Δpdr5::hisG, Δpdr10::hisG, Δpdr11::hisG, Δycf1::hisG, Δpdr3::hisG, Δpdr15::hisG, Δybt1::* kanMX)	This study
AD-RP-Mlt1p-GFP	AD-RP cells harbouring *MLT1* ORF fused with GFP integrated at *PDR5* locus	This study
AD-RP-K710A Mlt1p-GFP	AD-RP-Mlt1p-GFP cells harbouring K710A mutation in *MLT1* ORF and integrated at *PDR5* locus	This study

AD-RP-Mlt1p-HIS	AD-RP cells harbouring *MLT1* ORF fused with His tag integrated at *PDR5* locus	This study
AD-RP-K710A Mlt1p-HIS	AD-RP-Mlt1p-HIS cells harbouring K710A mutation in *MLT1* ORF and integrated at *PDR5* locus	This study

A

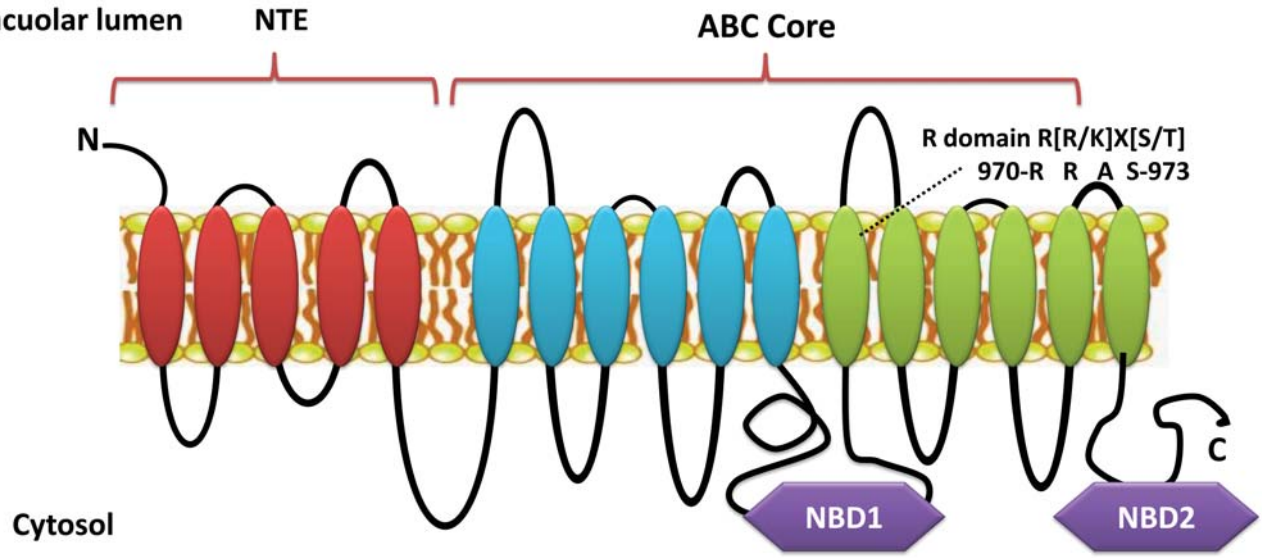

B

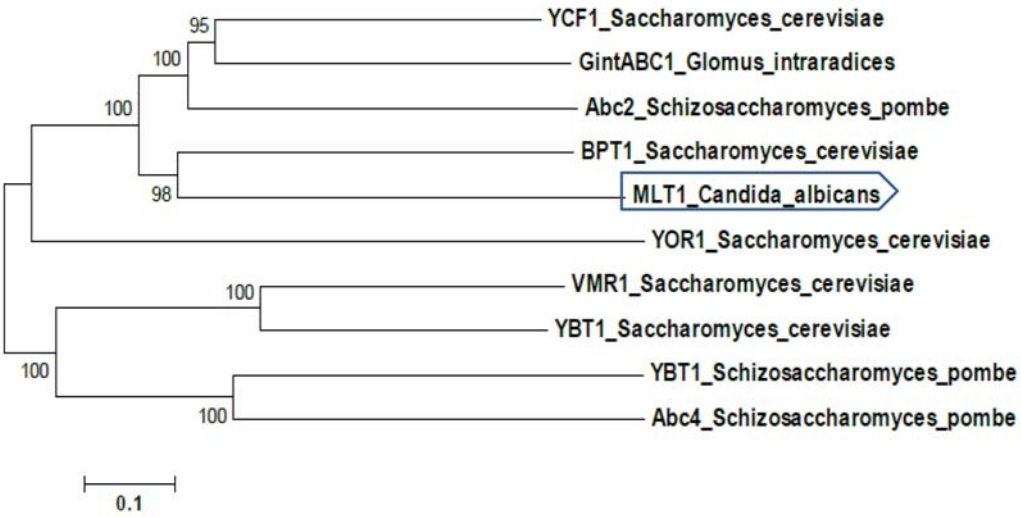

C

	CaMlt1 Identity	CaMlt1 Similarity	Gaps
ScYbt1	30%	48%	10%
ScBpt1	39%	59%	6%
ScYcf1	40%	46%	8%

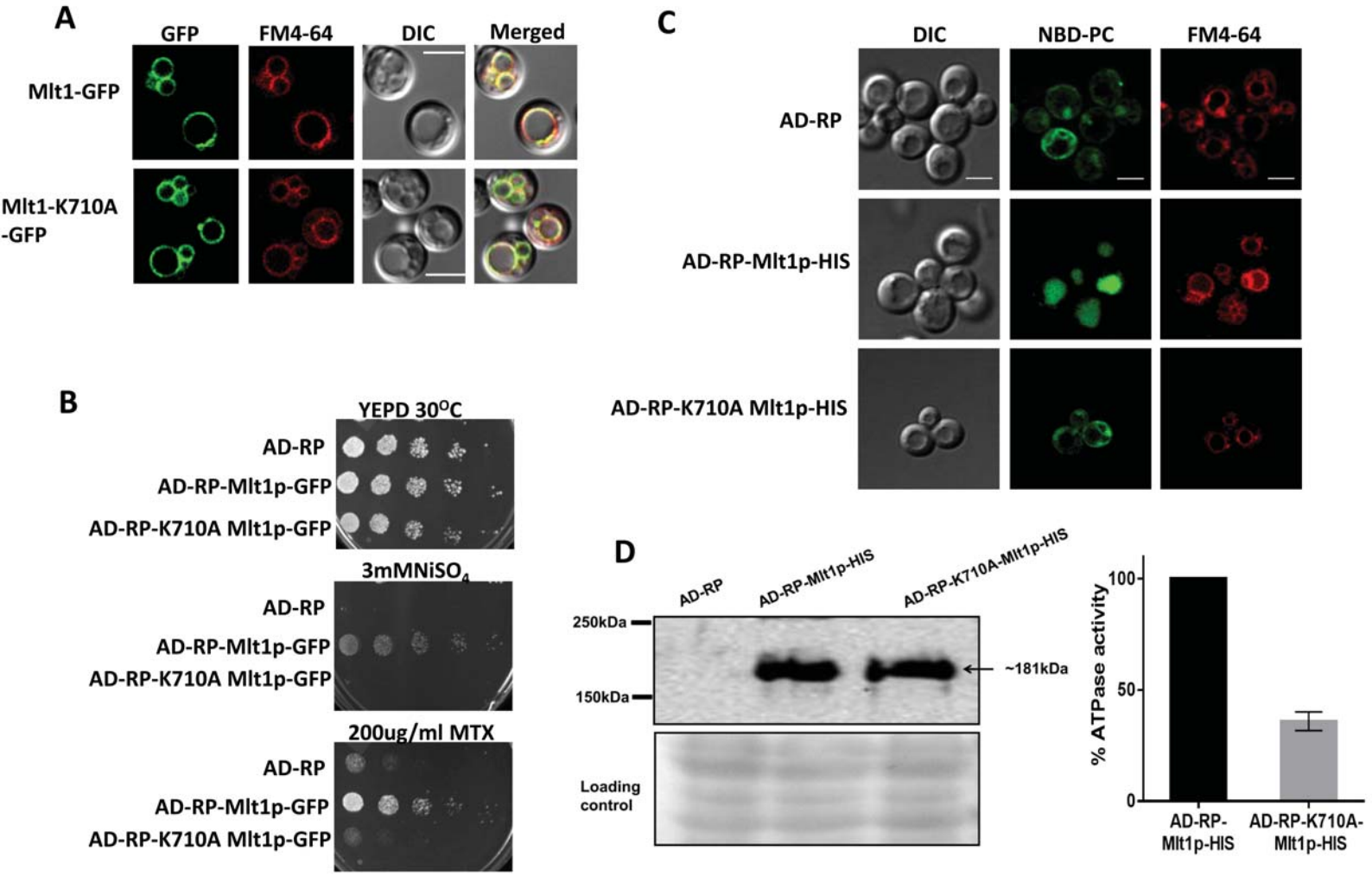
A
GFP
FM4-64
DIC
Merged
Mlt1-GFP
Mlt1-K710A -GFP
B
YEPD 30°C
AD-RP
AD-RP-Mlt1p-GFP
AD-RP-K710A Mlt1p-GFP
3mMNiSO4
AD-RP
AD-RP-Mlt1p-GFP
AD-RP-K710A Mlt1p-GFP
200ug/ml MTX
AD-RP
AD-RP-Mlt1p-GFP
AD-RP-K710A Mlt1p-GFP
C
DIC
NBD-PC
FM4-64
AD-RP
AD-RP-Mlt1p-HIS
AD-RP-K710A Mlt1p-HIS
D
AD-RP
AD-RP-Mlt1p-HIS
AD-RP-K710A-Mlt1p-HIS
250kDa
150kDa
~181kDa
Loading control
% ATPase activity
100
50
0
AD-RP-Mlt1p-HIS
AD-RP-K710A-Mlt1p-HIS

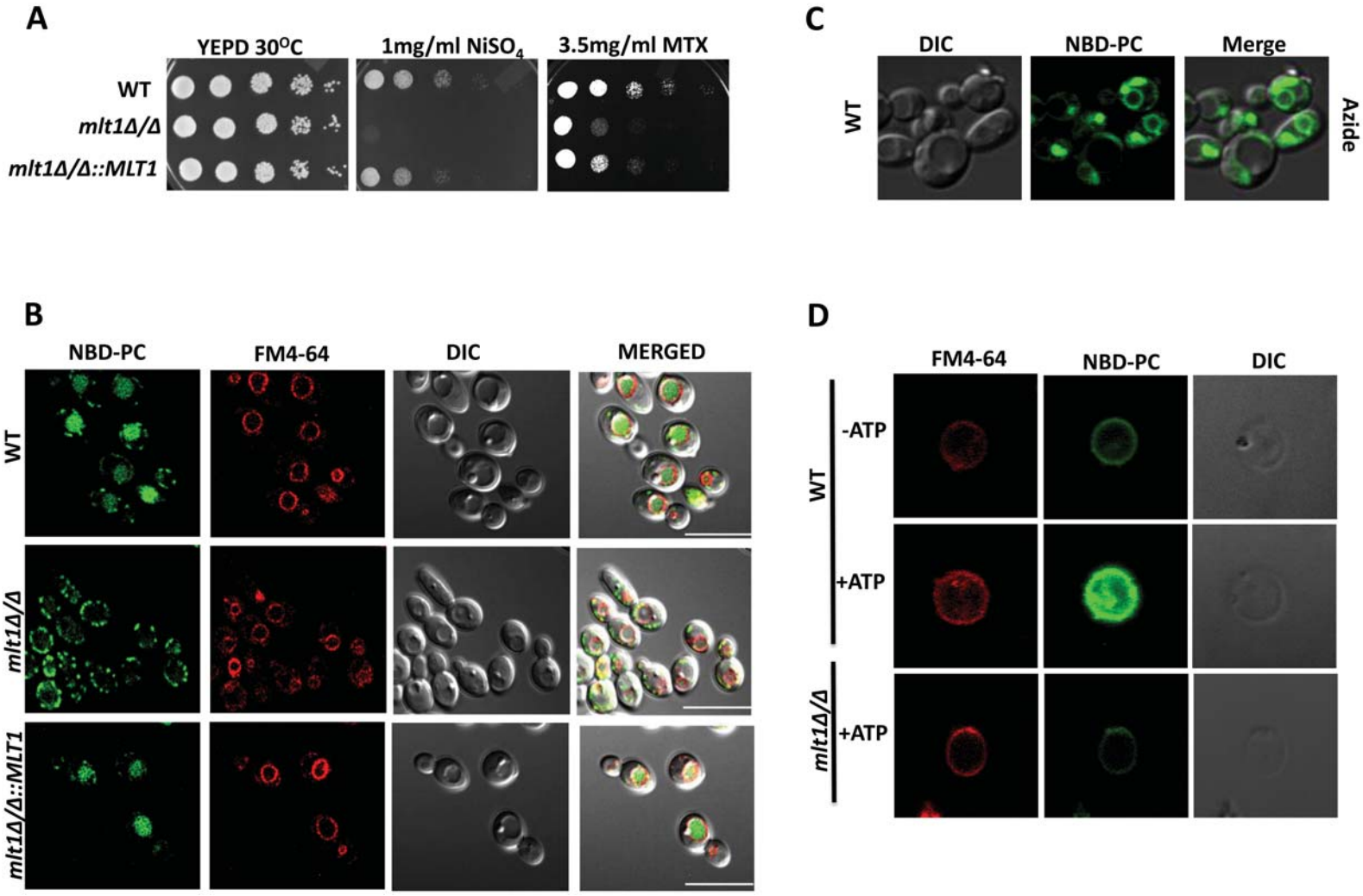
A
YEPD 30°C
1mg/ml NiSO4
3.5mg/ml MTX
WT
mlt1Δ/Δ
mlt1Δ/Δ::MLT1
C
DIC
NBD-PC
Merge
WT
Azide
B
NBD-PC
FM4-64
DIC
MERGED
WT
mlt1Δ/Δ
mlt1Δ/Δ::MLT1
D
FM4-64
NBD-PC
DIC
WT
-ATP
+ATP
mlt1Δ/Δ
+ATP

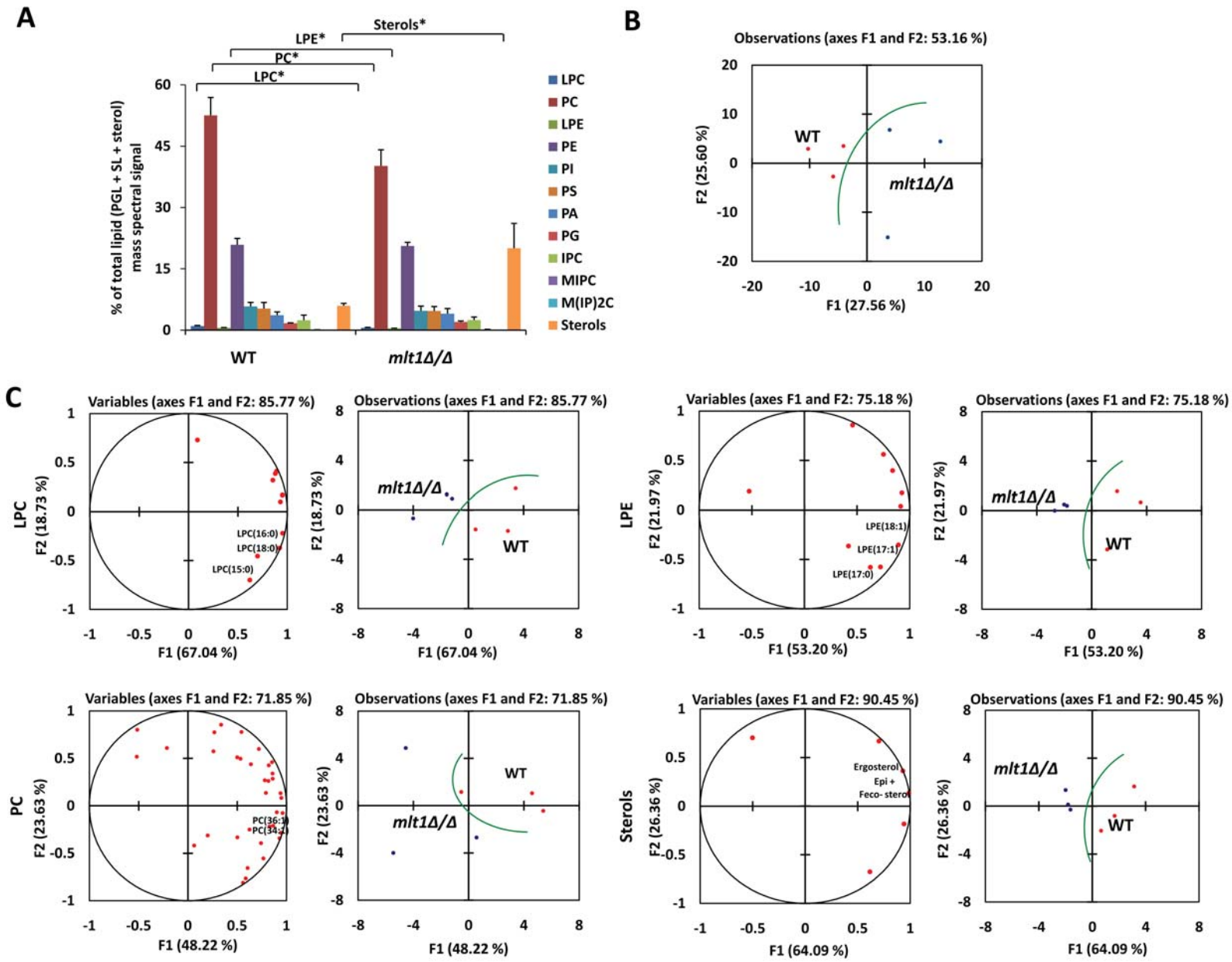
A
Sterols*
LPE*
PC*
LPC*
% of total lipid (PGL + SL + sterol) mass spectral signal
60
45
30
15
0
WT
mlt1Δ/Δ
LPC
PC
LPE
PE
PI
PS
PA
PG
IPC
MIPC
M(IP)2C
Sterols
B
Observations (axes F1 and F2: 53.16 %)
F2 (25.60 %)
F1 (27.56 %)
WT
mlt1Δ/Δ
C
Variables (axes F1 and F2: 85.77 %)
Observations (axes F1 and F2: 85.77 %)
LPC
F2 (18.73 %)
F1 (67.04 %)
LPC(16:0)
LPC(18:0)
LPC(15:0)
mlt1Δ/Δ
WT
Variables (axes F1 and F2: 75.18 %)
Observations (axes F1 and F2: 75.18 %)
LPE
F2 (21.97 %)
F1 (53.20 %)
LPE(18:1)
LPE(17:1)
LPE(17:0)
Variables (axes F1 and F2: 71.85 %)
Observations (axes F1 and F2: 71.85 %)
PC
F2 (23.63 %)
F1 (48.22 %)
PC(36:1)
PC(34:1)
Variables (axes F1 and F2: 90.45 %)
Observations (axes F1 and F2: 90.45 %)
Sterols
F2 (26.36 %)
F1 (64.09 %)
Ergosterol
Epi +
Feco- sterol

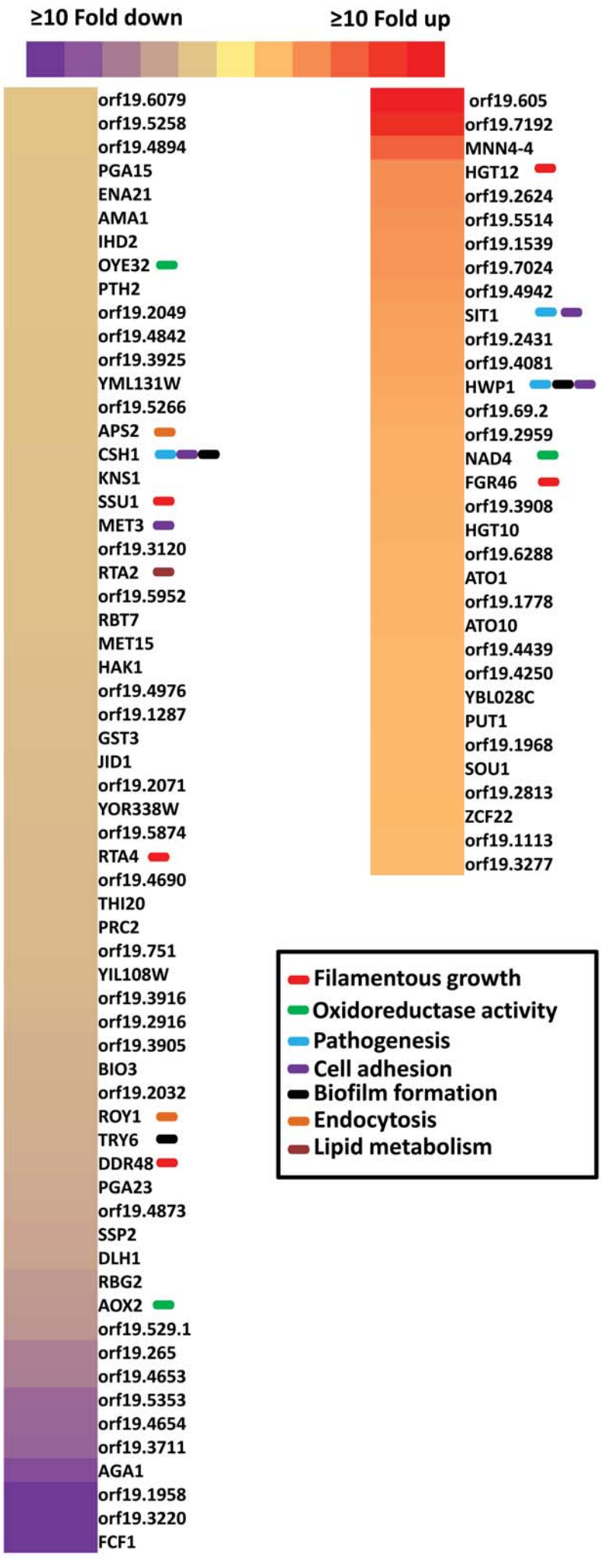
≥10 Fold down
≥10 Fold up
orf19.6079
orf19.5258
orf19.4894
PGA15
ENA21
AMA1
IHD2
OYE32
PTH2
orf19.2049
orf19.4842
orf19.3925
YML131W
orf19.5266
APS2
CSH1
KNS1
SSU1
MET3
orf19.3120
RTA2
orf19.5952
RBT7
MET15
HAK1
orf19.4976
orf19.1287
GST3
JID1
orf19.2071
YOR338W
orf19.5874
RTA4
orf19.4690
THI20
PRC2
orf19.751
YIL108W
orf19.3916
orf19.2916
orf19.3905
BIO3
orf19.2032
ROY1
TRY6
DDR48
PGA23
orf19.4873
SSP2
DLH1
RBG2
AOX2
orf19.529.1
orf19.265
orf19.4653
orf19.5353
orf19.4654
orf19.3711
AGA1
orf19.1958
orf19.3220
FCF1
orf19.605
orf19.7192
MNN4-4
HGT12
orf19.2624
orf19.5514
orf19.1539
orf19.7024
orf19.4942
SIT1
orf19.2431
orf19.4081
HWP1
orf19.69.2
orf19.2959
NAD4
FGR46
orf19.3908
HGT10
orf19.6288
ATO1
orf19.1778
ATO10
orf19.4439
orf19.4250
YBL028C
PUT1
orf19.1968
SOU1
orf19.2813
ZCF22
orf19.1113
orf19.3277
Filamentous growth
Oxidoreductase activity
Pathogenesis
Cell adhesion
Biofilm formation
Endocytosis
Lipid metabolism

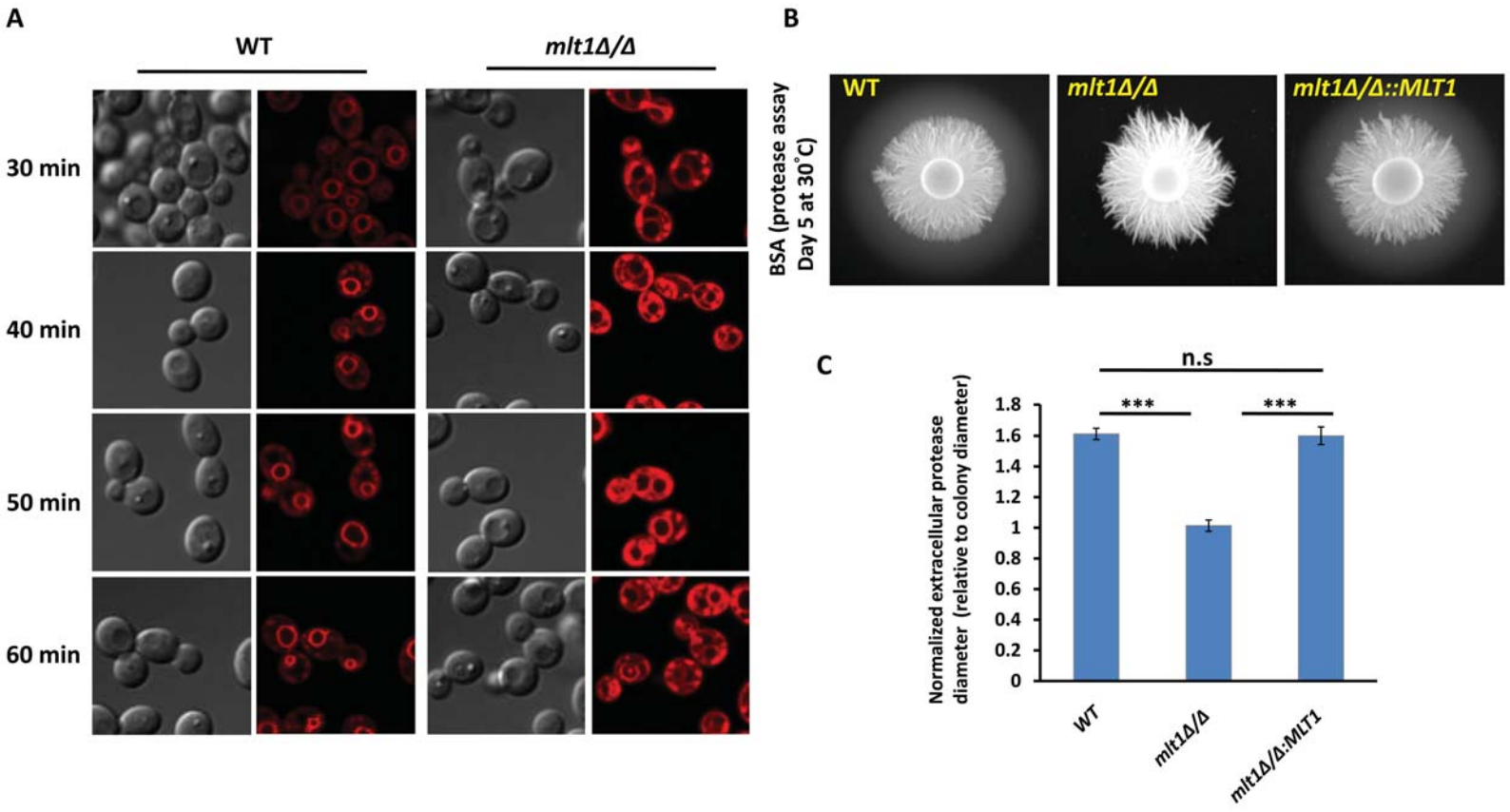
A
WT
mlt1Δ/Δ
30 min
40 min
50 min
60 min
B
BSA (protease assay
Day 5 at 30°C)
WT
mlt1Δ/Δ
mlt1Δ/Δ::MLT1
C
n.s
***
***
Normalized extracellular protease
diameter (relative to colony diameter)
1.8
1.6
1.4
1.2
1
0.8
0.6
0.4
0.2
0
WT
mlt1Δ/Δ
mlt1Δ/Δ:MLT1

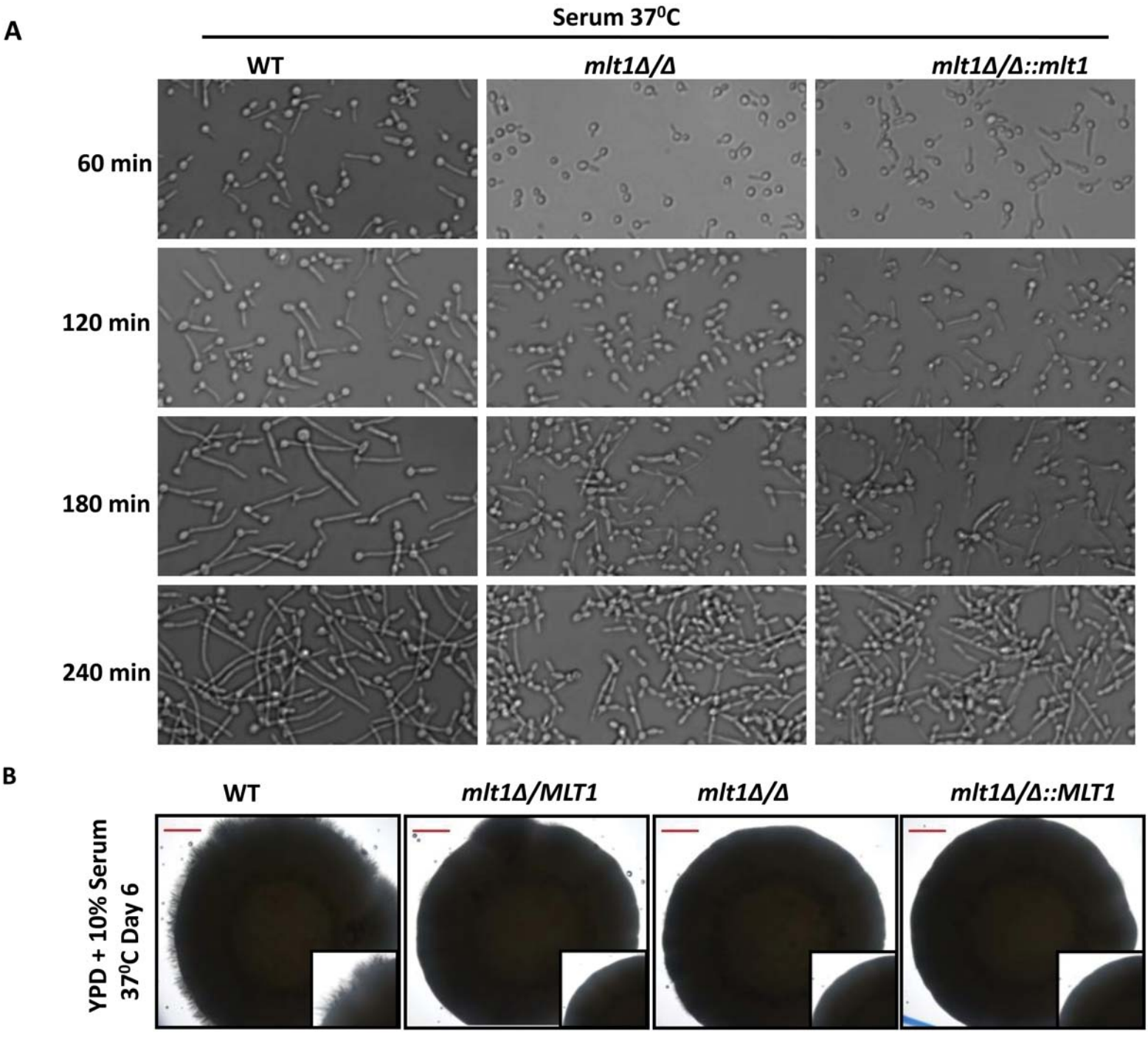
A
Serum 37⁰C
WT
mlt1Δ/Δ
mlt1Δ/Δ::mlt1
60 min
120 min
180 min
240 min
B
WT
mlt1Δ/MLT1
mlt1Δ/Δ
mlt1Δ/Δ::MLT1
YPD + 10% Serum
37⁰C Day 6

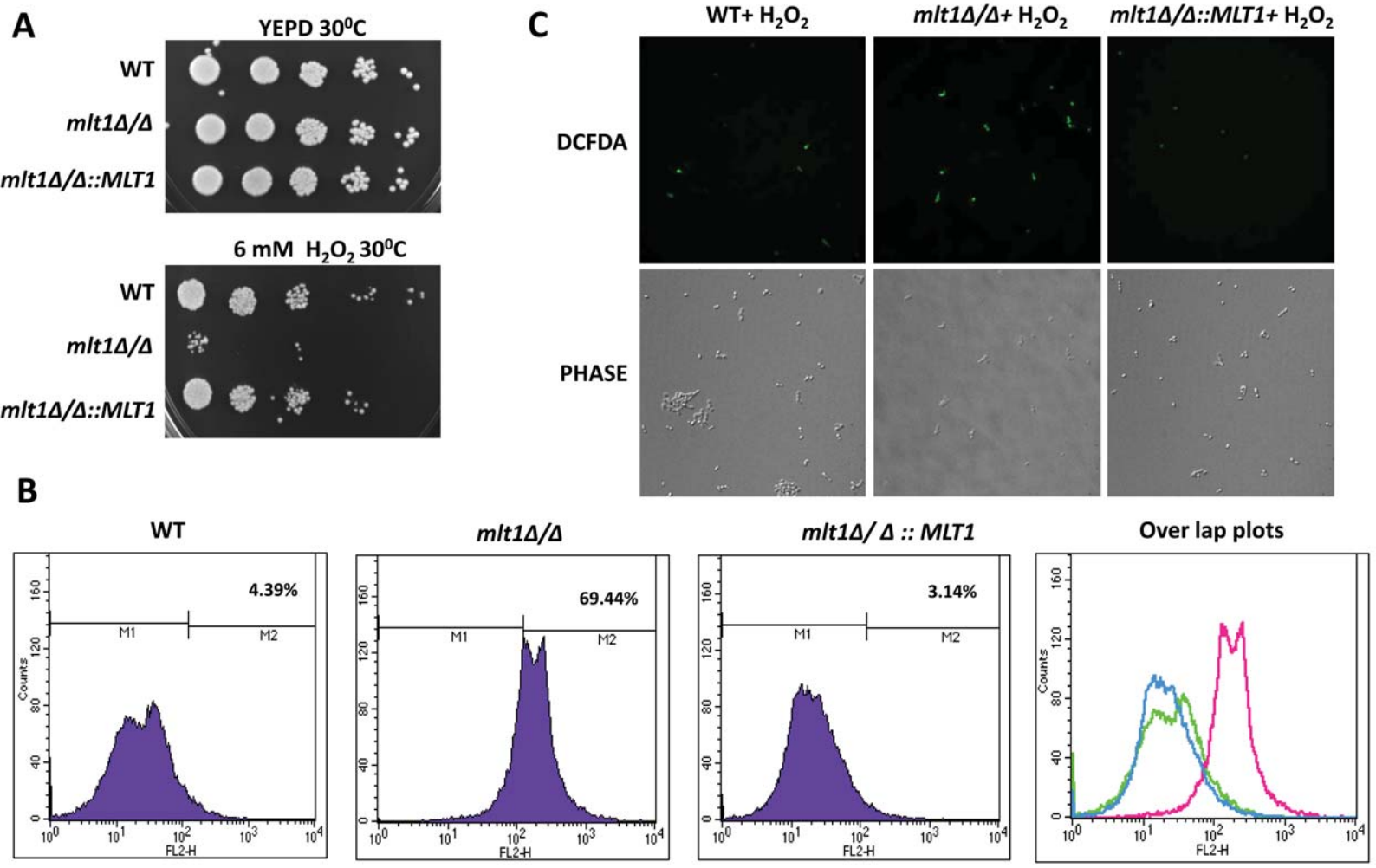
A
YEPD 30⁰C
WT
mlt1Δ/Δ
mlt1Δ/Δ::MLT1
6 mM H2O2 30⁰C
WT
mlt1Δ/Δ
mlt1Δ/Δ::MLT1
C
WT+ H2O2
mlt1Δ/Δ+ H2O2
mlt1Δ/Δ::MLT1+ H2O2
DCFDA
PHASE
B
WT
mlt1Δ/Δ
mlt1Δ/ Δ :: MLT1
Over lap plots
4.39%
69.44%
3.14%
M1
M2
Counts
FL2-H

A

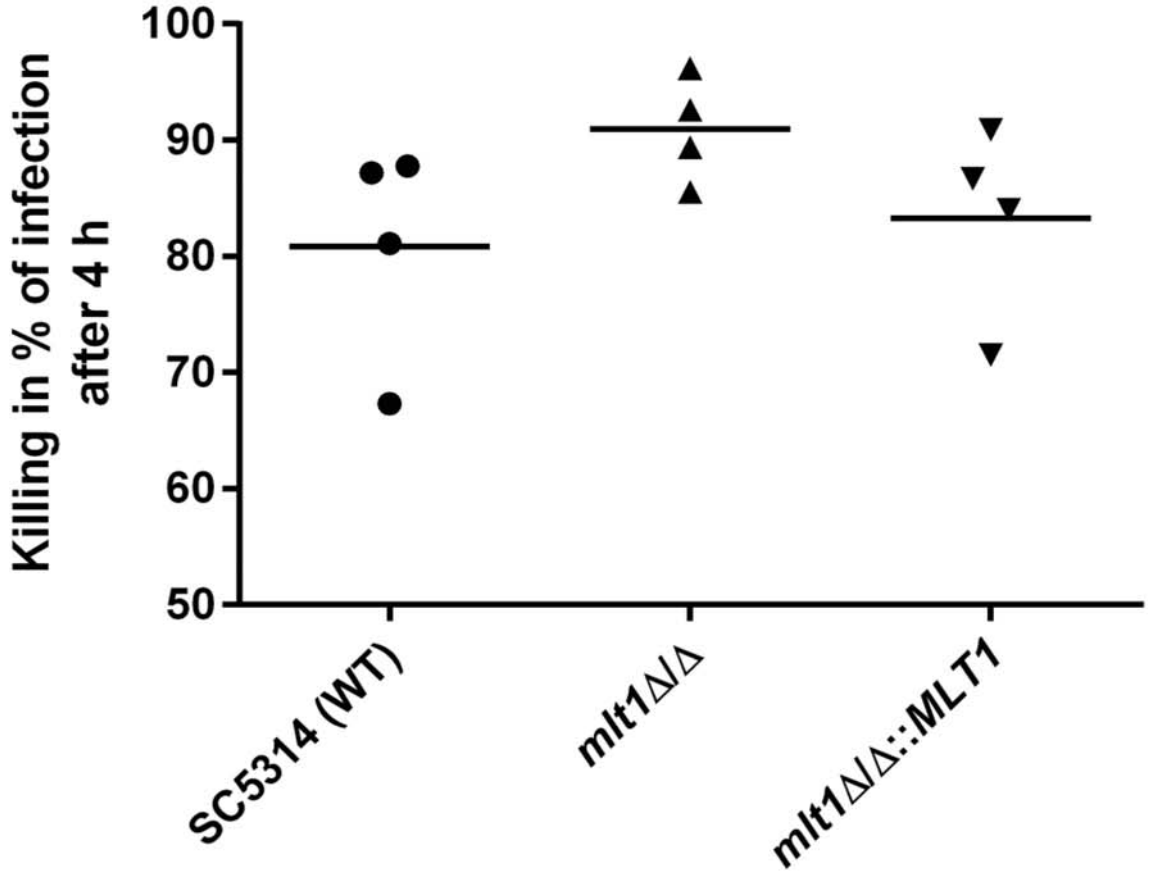
Killing in % of infection after 4 h
100
90
80
70
60
50
SC5314 (WT)
mlt1Δ/Δ
mlt1Δ/Δ::MLT1

B

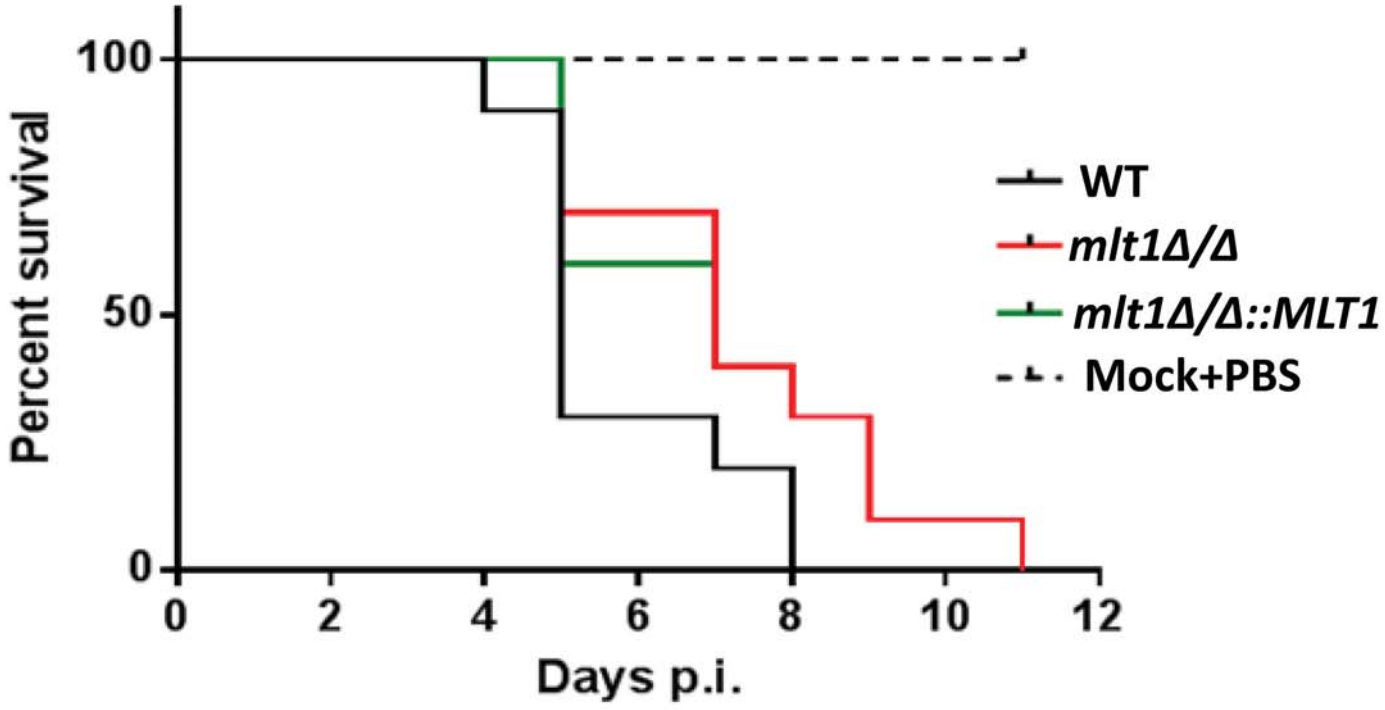
Percent survival
100
50
0
0
2
4
6
8
10
12
Days p.i.
WT
mlt1Δ/Δ
mlt1Δ/Δ::MLT1
Mock+PBS

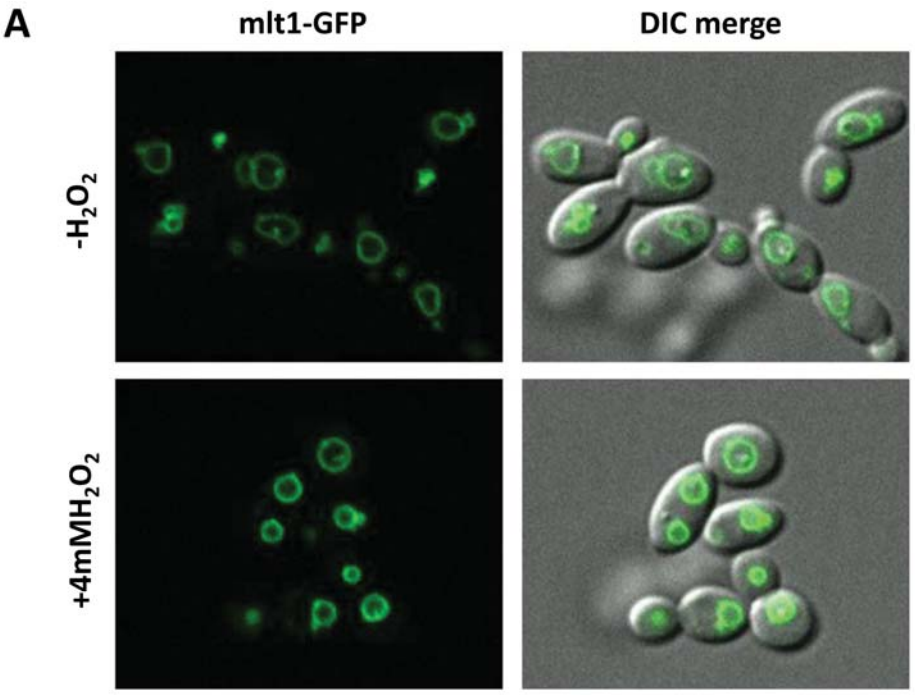
A
mlt1-GFP
DIC merge
-H2O2
+4mMH2O2

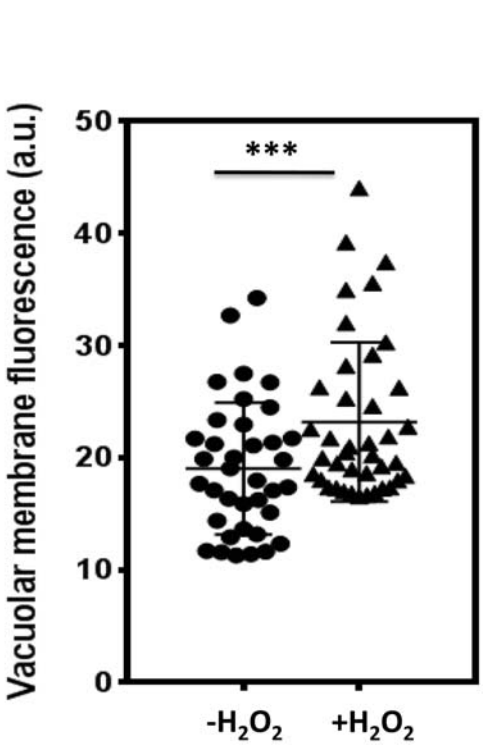
B
Vacuolar membrane fluorescence (a.u.)
50
40
30
20
10
0
***
-H2O2
+H2O2

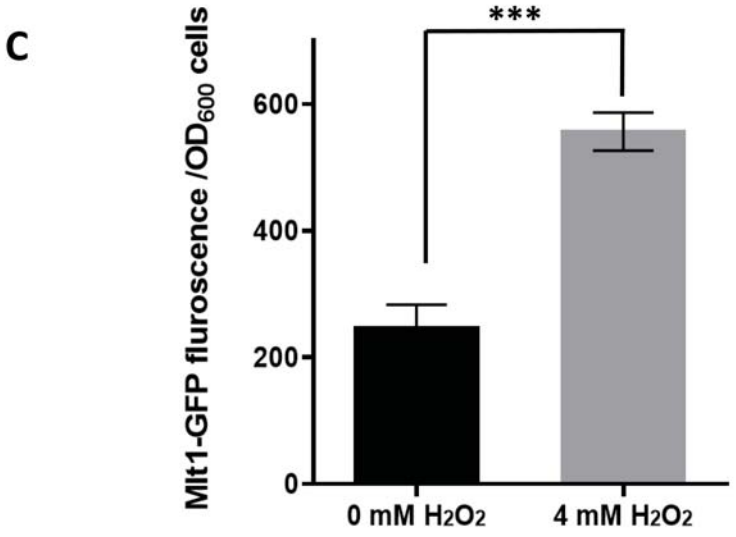
C
Mlt1-GFP fluroscence /OD600 cells
600
400
200
0
***
0 mM H2O2
4 mM H2O2

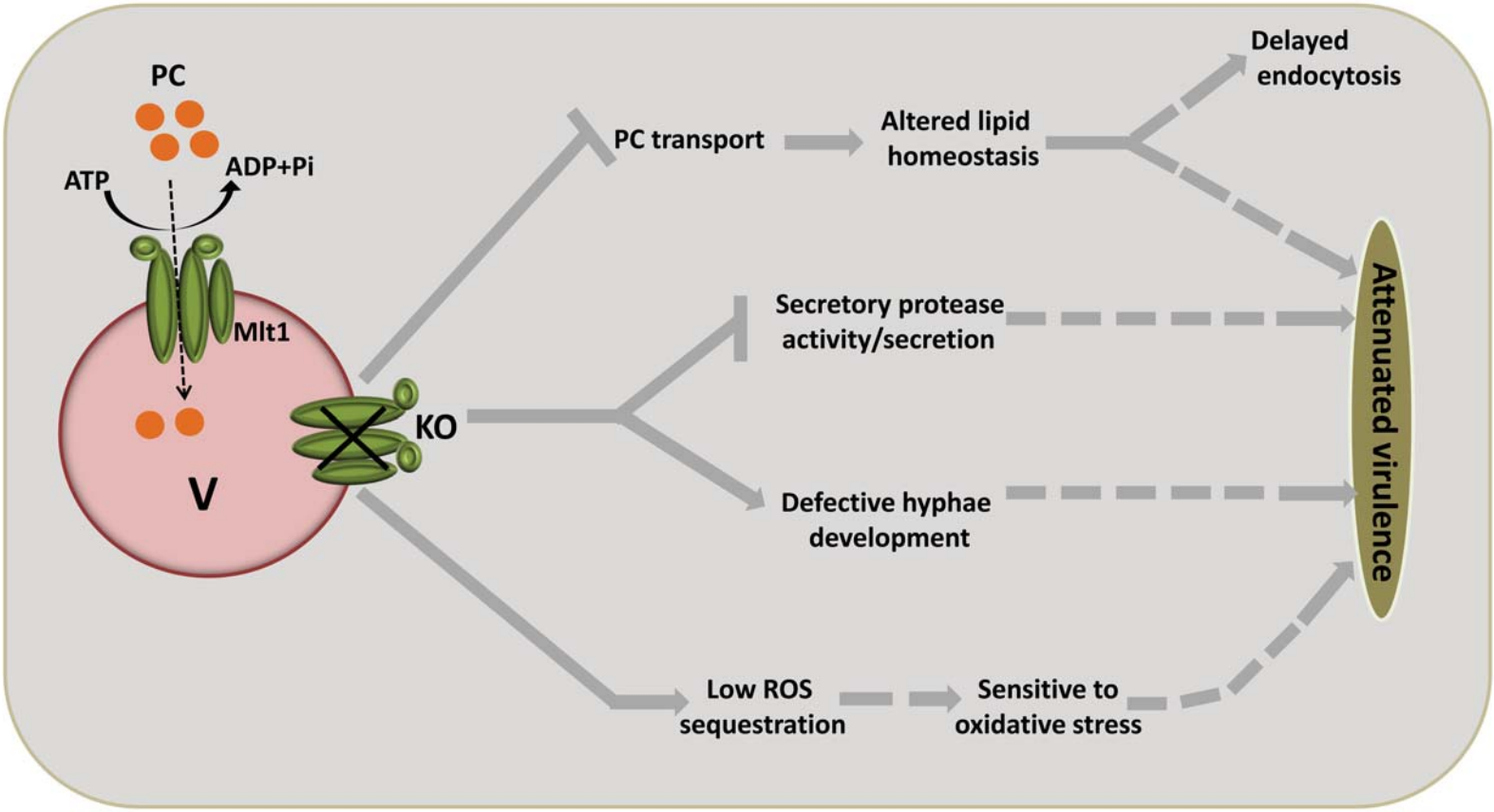
PC
ATP
ADP+Pi
Mlt1
V
KO
PC transport
Altered lipid homeostasis
Delayed endocytosis
Secretory protease activity/secretion
Defective hyphae development
Low ROS sequestration
Sensitive to oxidative stress
Attenuated virulence